fishes

MDPI

Article

Simulating the Effects of Temperature and Food Availability on True Soles (*Solea* spp.) Early-Life History Traits: A Tool for Understanding Fish Recruitment in Future Climate Change Scenarios

Adriana E. Sardi [1,†], José M. Moreira [2], Lisa Omingo [3], Xavier Cousin [4], Marie-Laure Bégout [4], Manuel Manchado [3] and Nina Marn [5,6,*,†]

1 EPOC-LPTC, UMR 5805, CNRS, University of Bordeaux, 33400 Talence, France
2 MARETEC—Marine, Environment and Technology Center, LARSyS, Instituto Superior Técnico, University of Lisbon, Av. Rovisco País 1, 1049-001 Lisboa, Portugal
3 IFAPA Centro El Toruño, Junta de Andalucía, Camino Tiro Pichón s/n, 11500 El Puerto de Santa Maria, Spain
4 MARBEC, Univ Montpellier, CNRS, Ifremer, IRD, INRAE, 34250 Palavas-Les-Flots, France
5 Division for Marine and Environmental Research, Rudjer Boskovic Institute, Bijenicka Cesta 54, 10002 Zagreb, Croatia
6 School of Biological Sciences, University of Western Australia, 35 Stirling Highway, Perth, WA 6009, Australia
* Correspondence: nmarn@irb.hr
† These authors contributed equally to this work.

Abstract: Research on recruitment variability has gained momentum in the last years, undoubtedly due to the many unknowns related to climate change impacts. Knowledge about recruitment—the process of small, young fish transitioning to an older, larger life stage—timing and success is especially important for commercial fish species, as it allows predicting the availability of fish and adapting fishing practices for its sustainable exploitation. Predicting tools for determining the combined effect of temperature rise and food quality and quantity reduction (two expected outcomes of climate change) on early-life history traits of fish larvae are valuable for anticipating and adjusting fishing pressure and policy. Here we use a previously published and validated dynamic energy budget (DEB) model for the common sole (*Solea solea*) and adapt and use the same DEB model for the Senegalese sole (*S. senegalensis*) to predict the effects of temperature and food availability on *Solea* spp. early life-history traits. We create seven simulation scenarios, recreating RCP 4.5 and 8.5 Intergovernmental Panel on Climate Change (IPCC) scenarios and including a reduction in food availability. Our results show that temperature and food availability both affect the age at metamorphosis, which is advanced in all scenarios that include a temperature rise and delayed when food is limited. Age at puberty was also affected by the temperature increase but portrayed a more complex response that is dependent on the spawning (batch) period. We discuss the implications of our results in a climate change context.

Keywords: climate change; dynamic energy budget theory; early-life stages; flatfish; food availability; recruitment

check for updates

Citation: Sardi, A.E.; Moreira, J.M.; Omingo, L.; Cousin, X.; Bégout, M.-L.; Manchado, M.; Marn, N. Simulating the Effects of Temperature and Food Availability on True Soles (*Solea* spp.) Early-Life History Traits: A Tool for Understanding Fish Recruitment in Future Climate Change Scenarios. *Fishes* **2023**, *8*, 68. https://doi.org/10.3390/fishes8020068

Academic Editor: Carlotta Mazzoldi

Received: 28 December 2022
Revised: 13 January 2023
Accepted: 17 January 2023
Published: 22 January 2023

Copyright: © 2023 by the authors. Licensee MDPI, Basel, Switzerland. This article is an open access article distributed under the terms and conditions of the Creative Commons Attribution (CC BY) license (https://creativecommons.org/licenses/by/4.0/).

1. Introduction

Research on recruitment variability—here referred to as the process of small, young fish transitioning to an older, larger life stage—has gained momentum in the last years [1–3], undoubtedly due to the many unknowns related to climate change (CC) impacts [4,5]. For example, temperature-driven reduction in primary production in the oceans is altering the recycling cycles of nutrients [6], which impacts the diversity and nutritious quality of zooplankton communities and consequently supports a smaller biomass of higher trophic levels, the overall result being warmer and nutrient poorer oceans [7]. The impacts of temperature-induced changes in phenology—studying the timing of recurring biological

events and how these are influenced by climate [8]—are hard to predict and demonstrate, but phenological adaptations, i.e., shifts in the timing of seasonal events, have been reported for many planktonic and nektonic marine species, including fish [9–13].

Early transitional life stages of fish have strict environmental requirements for differentiation, metamorphosis, settlement, and growth. The environmental conditions can be used to determine healthy development and survival rates, which are very variable and often very low [14]. When the environmental requirements are not met, there are consequences at later life stages that could compromise the fitness of individuals and, thus, the health of populations. Compared with any other fish life stage, larvae will have the highest potential for growth, the highest weight-specific metabolic rates, and the highest sensitivity to environmental fluctuations and stressors [15,16]. As most processes determining the recruitment strength and the spatial distribution of fish populations occur during the planktonic stage of fishes, evaluation of ichthyoplankton remains a key element for fisheries assessment. Further, the survival of fish larvae directly influences future abundances of adult fish stocks, resulting in important interannual fluctuations in fish stock biomasses.

Understanding recruitment requires coupling physical and biological processes. The dominant recruitment mechanisms affecting fish larvae's growth and survival are environmental factors, such as temperature and salinity, prey (feed) availability, predation pressure, and "the bigger and faster" relationship, which proposes that a bigger fish will be faster to evade predators and thus have a higher survival probability [17]. All of these mechanisms may act together over the entire period—from egg to the pre-recruit juvenile and are essential determinants of the year-class strength, i.e., the number of fish spawned or hatched in a given year and their respective recruitment success. Simultaneously to these environmental factors, growth and development are affected by the physiological characteristics of the individuals. Mechanistic bioenergetic models like Dynamic Energy Budget (DEB) models combine information on an individual's physiology and ecology with information on environmental factors [18,19]. For example, growth is tightly linked to temperature, which in DEB models governs other physiological rates such as feeding, maintenance, and development [20,21]. In this sense, DEB models are a perfect tool to study the impact of environmental variability on, for example, the size and age at metamorphosis and puberty, which are relevant early life-history traits that affect fish recruitment.

Here we simulate the effect of future CC scenarios on fishes' early life-history traits, particularly focusing on larval growth and age at metamorphosis in two flatfish species, the common sole, *Solea solea*, and the Senegalese sole, *S. senegalensis*. Both flatfish species are aquatic resources of high commercial value, appreciated in Europe due to their flesh quality [22–24].

Soles have a complex life cycle with progressive lifestyles and ontogenetic habitat shifts. *S. solea* and *S. senegalensis* are both "r strategist" species and batch spawners, and as such, they are characterized by strong fecundity. In both species, temperature is the principal environmental cue triggering the spawning of hundreds of thousands of eggs with low survival rates [25,26]. Fertilized eggs and larvae are both pelagic, which enables wide dispersion but also exposes these early life stages to (variable) environmental factors, notably temperature and food abundance. Recently hatched larvae drift towards estuaries and coastal areas—their juvenile environment—while they undergo metamorphosis. Major ontogenic, morphological, physiological, and behavioral changes occur during metamorphosis [27] and are accompanied by a change of habitat and lifestyle (from pelagic to benthic). The duration of metamorphosis varies depending on temperature and food availability. In *S. solea*, the transition from hatching until complete metamorphosis —the complete larval stage— can last between 15 and 26 days, at 19 °C and 16 °C, respectively [28], whereas the Senegalese sole usually takes about 8 days to complete metamorphosis at 20 °C, although with a high variability depending on environmental and feed availability [29,30]. Fully metamorphosed juveniles change from a pelagic to a benthic lifestyle—a process known as settlement—colonizing estuaries and bays that act as nursery areas [31,32]. The residence time in the nursery areas depends on fish size and development status and is around two to four years. Once fish reach maturity, adults migrate offshore (a

few or up to hundreds of kilometers, depending on location) for spawning. They eventually return closer to the shore after the reproductive season to reach feeding grounds.

Environmental fluctuations strongly influence the spawning time, survival rates, egg and larval life history, the larval growth, development and dispersion process, and the transition from a pelagic to a benthic lifestyle [33]. For understanding the potential implications that (environmentally and thus CC-influenced) larval growth and development have for *Solea* spp. settlement and recruitment, we apply the species-specific DEB models to study the expected effects under future CC scenarios. Both species have three distinct life stages that characterize their development: a post-hatch pelagic larval phase, a juvenile benthic phase, and an adult benthic phase, so we decided to focus on two distinct life stage transitions: metamorphosis and puberty. We generate seven different temperature and food availability scenarios and study their effect on the growth and development of the early-life stages of these two flatfish species. We focus on larval stages as their sensitivity to CC might be further increased due to their high (mass-specific) metabolic rate, lower energy reserves, and the fact that they are less capable of migrating toward a suitable habitat [14], but we run our simulations until puberty is attained. Our hypothesis is that DEB model simulations will help identify the main effects of CC-induced changes in *Solea* spp. early-life-history traits when changes in food availability and temperature are forced into the models. Further, the effect of forcing variables should differ between spawning batches, which will have experienced different temperature exposure.

2. Materials and Methods

2.1. DEB Theory and Models

Dynamic Energy Budget (DEB) theory [18,20,21] focuses on energy—and mass—pathways in a (dynamic) environment, i.e., on energy and nutrient acquisition and subsequent utilization by an individual throughout its life cycle. DEB-based models describe the energy budgets of individual organisms, quantifying metabolism and the interaction of processes that constitute it, including feeding, maintenance, development or maturation, growth, reproduction, and aging. Temperature and food availability are often the main forcing variables in the model, and thus the way these environmental factors modify metabolism is considered explicitly. Further, dynamic energy budgets follow the changes of these fluxes during an organism's complete life cycle, translating the individual's physiological functions into a reduced number of differential equations and a dozen or so primary parameters. Most parameters are species-specific (see next section on model parameterization), but the rules for energy pathways are universal: energy is assimilated from food into energy reserves and then is mobilized (used) to fuel all metabolic processes, with maintenance having priority over growth and development (maturation) or reproduction. Life stage transitions, such as metamorphosis and puberty, are explicit maturity thresholds. Here, 'maturity' is one of the three main model state variables; the other two are 'energy reserve' and 'structure'. Combined, the three state variables completely describe a (juvenile) individual: maturity tracks its development or maturation, and reserve and structure its size. After attaining puberty, an additional state variable, 'reproductive buffer', can be used to track the size and model reproduction of adults. For the complete model description, including a list of state variables and corresponding equations, please see Appendix A.

2.2. Accounting for Temperature and Food Availability

Temperature and food availability are the two main forcing variables in the model, effectively translating the environmental conditions into physiological responses of studied individuals. For the conversion between food availability and perceived food (scaled functional response, f), we use the Holling type II functional response:

$$f = X/X_K + X, \quad (1)$$

where X is the food density and X_K is the half-saturation constant for that type of food. Because f is a saturating function, it can vary between 0 when no food is available (food deprivation), and 1 food is abundant (feeding *ad libitum*).

The correction for the effect of (water) temperature is done using the Arrhenius equation (Equation (1.2) in [20]) and is assumed to be the same for all metabolic rates (Section 1.2 in [20]). The rate at a given temperature T is then obtained as:

$$k(T) = c(T)\, k(T_{ref}), \quad (2)$$

where c(T) is the correction factor for a certain temperature T, and $k(T_{ref})$ is the rate at the reference temperature (T_{ref} = 293.15 K or 20 °C by convention [20]). Where appropriate, we used an extended 5- parameter temperature correction (pp. 21–22 in [20], [34]) to capture the fact that *S. senegalensis* might be experiencing suboptimally cold and *S. solea* suboptimally warm temperatures during simulations. The full temperature correction function is presented in Appendix A and is available as a pre-coded function tempcorr.m in the freely available Matlab package DEBtool_M [35], which was used for parameter estimation.

2.3. Model Parameterization for S. solea and S. senegalensis

The life cycle and ontogeny of both sole species (*S. solea* and *S. senegalensis*) can be described by the abj-type model, which includes a metabolic acceleration between birth and metamorphosis and accounts for the metamorphosis of flatfish species in their early life cycle [36,37]. The metabolic metamorphosis is assumed to coincide with the physical metamorphosis (the process of eye migration and head remodeling), with "age and size at metamorphosis" (in the DEB model) corresponding to the properties of the fish at the end of physical metamorphosis, i.e., head remodeling.

We decided to use the same abj-type models for *S. solea* and *S. senegalensis*. The models share the same assumptions and model setup, but they differ in species-specific parameter values. For parameterization of the *S. solea* model, we focused on the study by Mounier et al. [38] and on the latest available Add-my-pet entry (Teal, AmP *Solea solea*, version 2015/08/28). Both of these versions of the *S. solea* models were parameterized using the AmP tool setup [39], so we merged the scripts and complemented the data with data on larval growth and development at several temperatures [40,41]. We then re-estimated parameters to obtain a comprehensive parameter set able to describe all data. For *S. senegalensis*, a DEB model was parameterized using data on life history (age and size at life events) and other data, such as growth curves at a known temperature, from published and unpublished sources. All parameter estimation was performed in Matlab using AmPtool and DEBtool [35,39,42]. The fits of model predictions to data used for model parameterization and all DEB parameter estimates for *S. solea* and *S. senegalensis* are presented in Appendix B. The complete code is freely available in the AmP collection by searching for the species' name.

2.4. Models Validation

We validated the models using independent datasets on larval growth (from birth to metamorphosis) reared under controlled conditions of temperature and food availability (data from [43,44]). Briefly, datasets consist of regular length and dry weight measurements of larvae reared under laboratory conditions using polystyrene microplates with a cover as a housing system. This type of housing allowed for monitoring larvae growth, development, and survival at the individual level during the entire experiment, which lasted for seven (*S. solea*) or four (*S. senegalensis*) weeks. The experiment included two factors: rearing temperature (16 °C and 20 °C in *S. solea* and 17 °C, 20 °C, and 23 °C in *S. senegalensis*) and feeding regimes (three levels: high, medium, and low food, approximated by different feeding frequencies). For *S. solea*, the data on larvae length is available for every week of the experiment (7 measurements starting at age 8 dph). In contrast, for dry weight, four measurements are available, three corresponding to the first week and one for the last week. Biometric data on *S. senegalensis* were collected at three different times before placing the larvae in microplates (12 dph), at intermediate age (22 dph), and at the end of the experiment (32 dph).

For model validation, physiological (species-specific) parameters were fixed for both species, while the dataset-specific scaled food availability (f) was manually adjusted until a satisfactory fit between model predictions and data was obtained. The temperature was explicitly taken into account by correcting all rates to the corresponding temperature (Equation (2)).

2.5. Simulation Setup

All simulations were set in a hypothetical location based on the temperature characteristics of the west coast of France and Portugal, as both species can be found—at different abundances—in this geographical extension [26,45]. To mimic the natural life-history events and study potential sources of inter-individual variability, we simulated early, middle, and late spawning for each fish species: for *S. solea*, we used early January, early March, and early May, and for *S. senegalensis,* early May, mid-June, and early August corresponding to the observed spawning periods in this geographic area [45]. Spawning occurs on the continental shelf and is followed by "migration" of the eggs and then larvae towards estuaries which serve as nurseries [3,5,46,47]. We assumed the migration to last 30 days, approximately corresponding to completing 75% of larval development at the time larvae reach the target nurseries (Table S1 and methods in [3]). Larvae were assumed to feed during the migration but with lower efficacy, resulting in a slight reduction of the overall scaled functional response: f during migration was assumed to be 75% of the f experienced by fish outside of the migration period. We assumed that the migration itself does not incur any additional energetic costs.

In all simulations, food availability after the migration was assumed constant, and initial energy in an egg was dependent on the mother's condition at the time of egg-laying (maternal effect [20]). Simulation duration depended on the species and the simulated scenario, as the simulations lasted until individuals were predicted to reach puberty: for *S. solea*, this was approximately 2.5 years, and for *S. senegalensis,* between 7 and 10 years. As points of interest, we made note of the predicted age and size at (i) hatching, (ii) birth (mouth opening), (iii) end of metamorphosis (complete larval development), and (iv) puberty (sexual maturation). We also tracked the growth (in total length) as a function of time, with food and temperature as forcing variables. Results are presented until complete maturation because we assume fish then leave the estuaries and go to the coastal sea to reproduce. All simulations were performed using MATLAB R2017b.

We evaluated the effect of temperature and the effect of food availability. In total, seven scenarios were simulated (Table 1), with three spawning events (early-mid-late) in each: S1 (bXbT) baseline scenario of current temperature conditions and current estimated food availability; S2 (bT−X) and S3(bT+X): scenarios with baseline temperature and a 50% decrease (bT−X) or a 50% increase (bT+X) in food availability (X, see Equation (1)); S4 (+TbX) and S5 (++TbX): scenario with a 1.8 degree (+TbX) and scenario with a 3.7-degree temperature increase (++TbX) from baseline temperature (RCP 4.5 and RCP 8.5 respectively, (Intergovernmental Panel on Climate Change IPCC, 2014), with current food availability; S6(+T−X) and S7(++T−X): scenarios with a 1.8 degree and a 3.7-degree temperature increase, respectively, and a 50% decrease in food availability.

Table 1. List of simulated scenarios (S1–S7) designed to reflect potential changes in temperature (warming of 1.8 and 3.7 degrees—RCP 4.5 and RCP 8.5, respectively, IPCC, 2014), and decrease and increase in food availability, both relative to the baseline, i.e., current conditions. Current (baseline) temperature is assumed to reflect the average seasonal fluctuations in typical coastal sea and estuaries inhabited by soles (see subsection 'Temperature scenarios' of Methods), and the food availability (X) is assumed to result in scaled functional response f = 0.85 in both species. In each scenario, there are three spawning events: early, middle, and late, the timing of which depends on the species.

Food (X)/Temperature (T)	Current Food (bX): Baseline	Low Food (−X): 0.5 × Baseline	High Food (+X): 1.5 × Baseline
Current temperature (bT): baseline	S1 (bTbX)	S2 (bT−X)	S3 (bT+X)
RCP 4.5 (+T): bT + 1.8 degree increase	S4 (+TbX)	S6 (+T−X)	/
RCP 8.5 (++T): bT + 3.7 degree increase	S5 (++TbX)	S7 (++T−X)	/

2.6. Temperature

The temperature baseline for our hypothetical location was designed as a sine function with the minimum temperature at Julian day 45 in mid-January, and the maximum temperature at Julian day 227.5, in mid-August. The coastline baseline temperature (T_{sea}) ranged from 10 °C to 20 °C, based on average temperature ranges in several locations on the west coast of France and Portugal (seatemperature.org). The estuary baseline temperature (T_{estu}) ranged from 10 °C to 24 °C, based on the average minimum and maximum temperatures in the principal estuaries of the English Channel, the Bay of Biscay, and the Portuguese coast, including Seine, Gironde, and Tagus [48–52]. The simplified temperature functions are:

$$T_{sea}(t) = 5 \sin f_0((2\pi(t - 136.25))/365) + 15$$

$$T_{estu}(t) = 7 \sin f_0((2\pi(t - 136.25))/365) + 17$$

To mimic the fact that larvae are spawned on the continental shelf and then are transported towards estuaries, we considered it essential to include a gradual shift from coastal to estuary temperatures. Therefore, we computed a final temperature function based on the two previous sinusoidal functions for the sea and for the estuary, which we used to describe the evolution of temperature as the forcing variable of our simulations. The resulting temperature was determined by elapsed time as a proportion of the total migration duration (t_{mig} = 30 days [3,5,53]): as time progresses, this function gives less weight to sea temperature and more weight to estuary temperature:

$$T(t) = (1 - dt/t_{mig}) \times T_{sea}(t) + (dt/t_{mig}) \times T_{estu}(t)$$

2.7. Food Availability

For the baseline food conditions, a constant food level equivalent to a functional response of f = 0.85 was selected based on similar values estimated for other species in the wild [54–57]. The food abundance (X) corresponding to f = 0.85 was calculated using Equation (1). For the scenarios targeted at evaluating the effect of food availability on the growth and development of fish, the decrease by 50% (relative to the baseline) resulted in a functional response of f = 0.74, whereas the increase by 50% resulted in f = 0.9.

3. Results

3.1. Models Parameterization and Validation

The models nicely captured individual traits along the whole life-cycle of both sole species, with model predictions generally fitting the data well (see Appendix B for model fits and Table 2 for a summary of the model parameters used within this study). The relatively low values for the mean relative error (MRE), symmetric mean average error (SMAE), and the symmetric mean squared error (SMSE) in both species parametrization

supported the visual inspection of the model fits: *S. solea* MRE = 0.102, SMAE = 0.109, SMSE = 0.023; *S. senegalensis* MRE = 0.552, SMAE = 0.136, SMSE = 0.057.

Table 2. Summary of DEB parameter estimates for the common sole (*S. solea*) and the Senegalese sole (*S. senegalensis)* that were used for the simulations. Two parameters (v and $\{p_{Am}\}$) in the abj-model applied here increase their value between birth and metamorphosis (see Appendix A), so the final value is provided in brackets. The final parameter value is calculated by multiplying the initial value by s_M = 2.7942 (*S. solea)* or by s_M = 3.3472 (*S. senegalensis*), s_M calculated for *f* = *1.* Arrhenius parameters for the 5-parameter temperature correction (T_L, T_H, T_{AL}, T_L) were set manually. For a full list of parameters, please see Tables A3 and A5 in Appendix B.

Parameter	Symbol	*S. solea*	*S. senegalensis*	Unit
Arrhenius temperature	T_A	7980	6528	K
Maximum surface area specific assimilation rate	$\{p_{Am}\}$	282.195 (788.5219)	95.61 (320.05)	J/d·cm^2;
Energy conductance	v	0.06828 (0.1908)	0.0697 (0.2332)	cm/d
Allocation fraction to soma (kappa)	κ	0.782	0.8117	-
Volume specific somatic maintenance	$[p_M]$	31.22	22.83	J/d·cm^3
Specific cost for structure	$[E_G]$	5188	5230	J/cm^3
Maturity at hatching	E_H^h	0.1809	0.0552	J
Maturity at birth	E_H^b	0.3417	0.1671	J
Maturity at end of metamorphosis	E_H^j	7.49	6.309	J
Maturity at puberty	E_H^p	1.964×10^5	1.258×10^6	J
Shape coefficient for larvae	δ_{Me}	0.1578	0.221	-
Shape coefficient post-metamorphosis	δ_M	0.199	0.2235	-
Arrhenius temperature for high temperature extreme	T_{AH}	20,000	20,000	K
High temperature extreme	T_H	294.15 (21 °C)	301.15 (28 °C)	K
Arrhenius temperature for low temperature extreme	T_{AL}	18,000	18,000	K
Low temperature extreme	T_L	280.15 (7 °C)	283.15 (10 °C)	

The maturity levels at hatching, birth, and metamorphosis are estimated to be higher for *S. solea* than for *S. senegalensis* (Table 2). This can explain the observed faster development and maturation of *S. senegalensis* when data for the same temperatures are compared [41,58]. However, the maturity level at puberty is estimated to be higher for *S. senegalensis*, implying that *S. solea* starts allocating energy toward reproduction sooner.

Other primary parameters imply a somewhat higher assimilation potential ($\{\dot{p}_{Am}\}$) for *S. solea*, coupled with a higher specific maintenance cost ($[\dot{p}_M]$). With a similar specific cost for structure ($[E_G]$) and allocation fraction to the soma (κ), we assume that the growth rates of the two species would not drastically differ, especially after final parameter values have been attained (post-acceleration). A notable difference is in the energy conductance ($\dot{v}$), which starts at a similar value at the larval phase (birth) but undergoes a more drastic acceleration (by a factor s_M = 3.34) in *S. senegalensis*. This, combined with the lower maturity thresholds mentioned earlier, contributes to the faster life cycle of the Senegalese sole and would result in faster growth compared with that of the common sole.

A higher Arrhenius temperature estimated for *S. solea* could be linked to the fact that parameterization of *S. solea* included a larger proportion of larval data, compared with *S. senegalensis*¸a point to which we come back in the discussion. Interestingly, the larval shape coefficient is similar to that for metamorphosized *S. senegalensis*, implying a negligible change in (metabolically relevant) shape; this could be a computational artifact.

3.2. Model Validation

DEB model growth predictions were able to capture the observations (data from [43,44]) while explicitly accounting for experimental temperature and manually adjusting the value of f to best match the observations (Figures 1 and 2). All other parameters were kept fixed at values listed in Table 2. For *S. solea*, the best fit to the data for the *ad libitum* treatment was obtained by setting the f parameter to 0.18 (Figure 1). For larvae at MediumFood and LowFood treatments, the f values were 0.15 and 0.10, respectively. For *S. senegalensis*, the f values were 0.4, 0.45, and 0.55, for larvae that were fed with low, medium and high frequency (Figure 2). We hypothesize these relatively low values implied for f in the discussion.

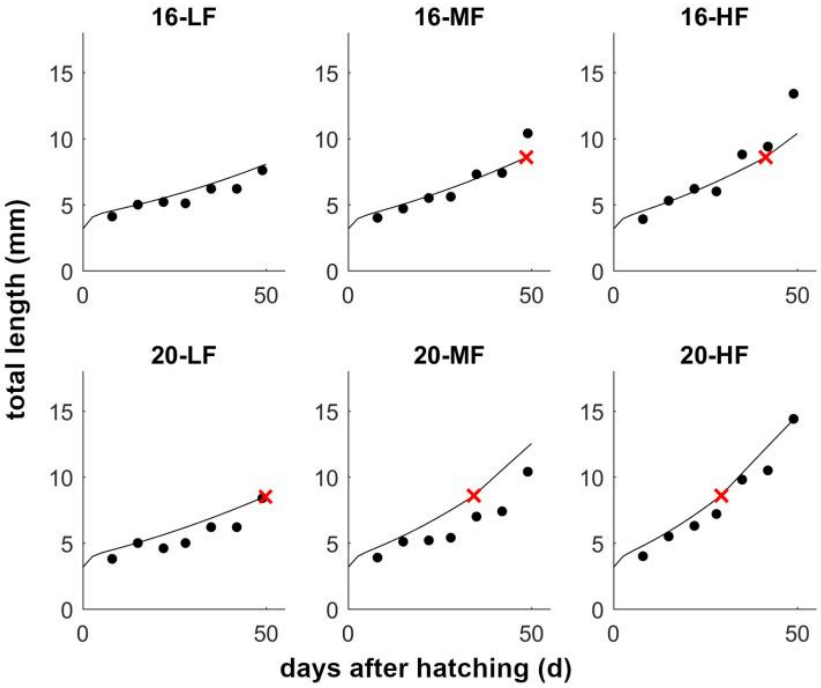


Figure 1. Model validation for *S. solea*. Larvae length (points) and DEB model larval growth predictions (lines) for *S. solea* larvae reared at three food availabilities (HighFood, HF; MediumFood, MF and LowFood, LF) and two constant temperatures (16 °C and 20 °C). Red X in the panels (where present) marks the end of metamorphosis as predicted by the model. Experimental conditions were modeled as follows: temperature for incubation 13 °C, hatching to birth: 16 °C, after birth: 16 °C (top row) or 20 °C (lower row). Temperature switches in the simulations are linked to life stage (maturity), not time. Size at birth will depend on the scaled food availability (f) experienced by the mother (f = 0.5), while subsequent growth will depend on experimental conditions (food and temperature) experienced by the larvae. Experimental f for larvae corresponds to feeding regimes: f_{LF} = 0.1, f_{MF} = 0.15, f_{HF} = 0.18. All f values were adjusted manually. Physiological parameters were kept fixed at values listed in Table 2.

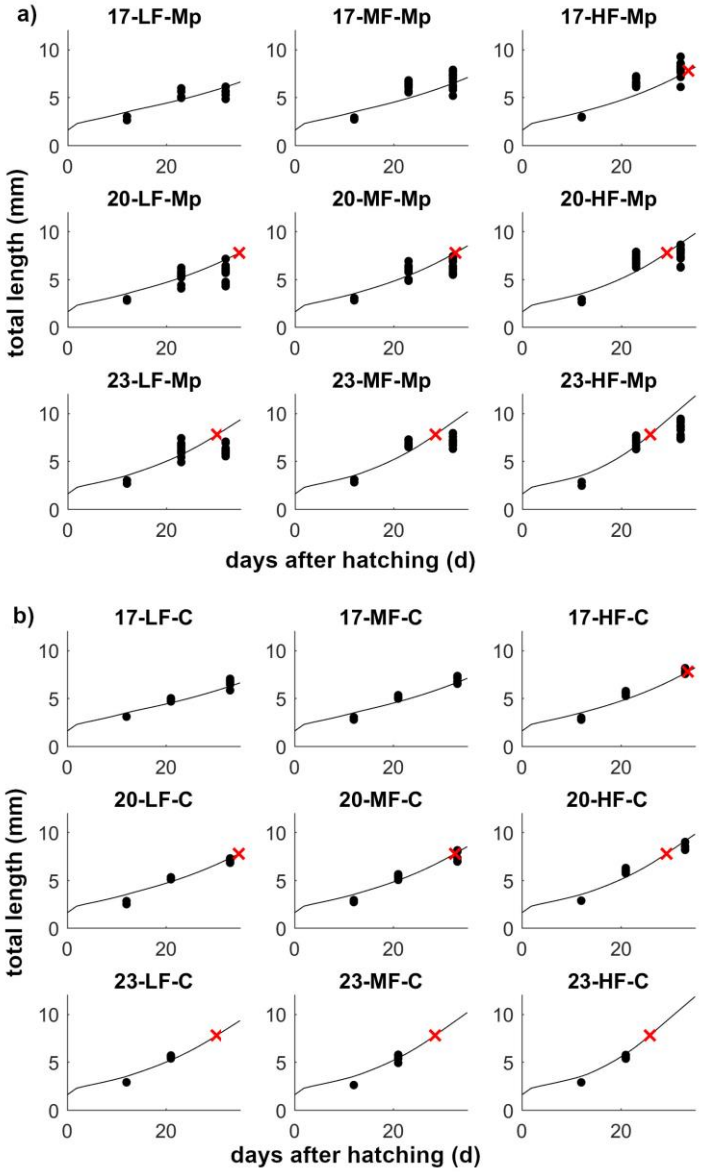


Figure 2. Model validation for *S. senegalensis*. Larvae length (points) and DEB model larval growth predictions (lines) for *S. senegalensis* larvae reared at three food availabilities (HighFood, HF; MediumFood, MF and LowFood, LF) and three constant temperatures (17 °C, 20 °C, and 23 °C). (**a**) Mp-microplates (individual fish); (**b**) C—containers. Red X in the panels (where present) marks the end of metamorphosis as predicted by the model. Experimental conditions were modeled as follows: temperature for incubation and first 12 days of rearing: 17 °C, afterward: 17 °C (top row), 20 °C (middle row), or 23 °C (bottom row). Temperature switches in the experimental simulations are linked to time. Size at birth will depend on the scaled food availability (f) experienced by the mother (f = 1), while subsequent growth will depend on experimental conditions (food and temperature) experienced by the larvae. Experimental f for larvae switches on day 12 from the initial f_{EXP} = 0.6 to treatment-specific: f_{LF} = 0.4, f_{MF} = 0.45, f_{HF} = 0.55. All f values were adjusted manually. Physiological parameters were kept fixed at values listed in Table 2.

3.3. Simulation Results

3.3.1. Temperature Increase Is Speeding Up the Development and Thus Reducing the Stage Duration

The stage duration, i.e., the time elapsed from one life event to the next one, decreased in both species within the simulation scenarios experiencing higher temperature (S4: +TbX

and S5: ++TbX), higher food availability (S3:bT+X), and even lower food availability if combined with a temperature increase (S6:+T−X and S7:++T−X) (Figures 3 and 4).

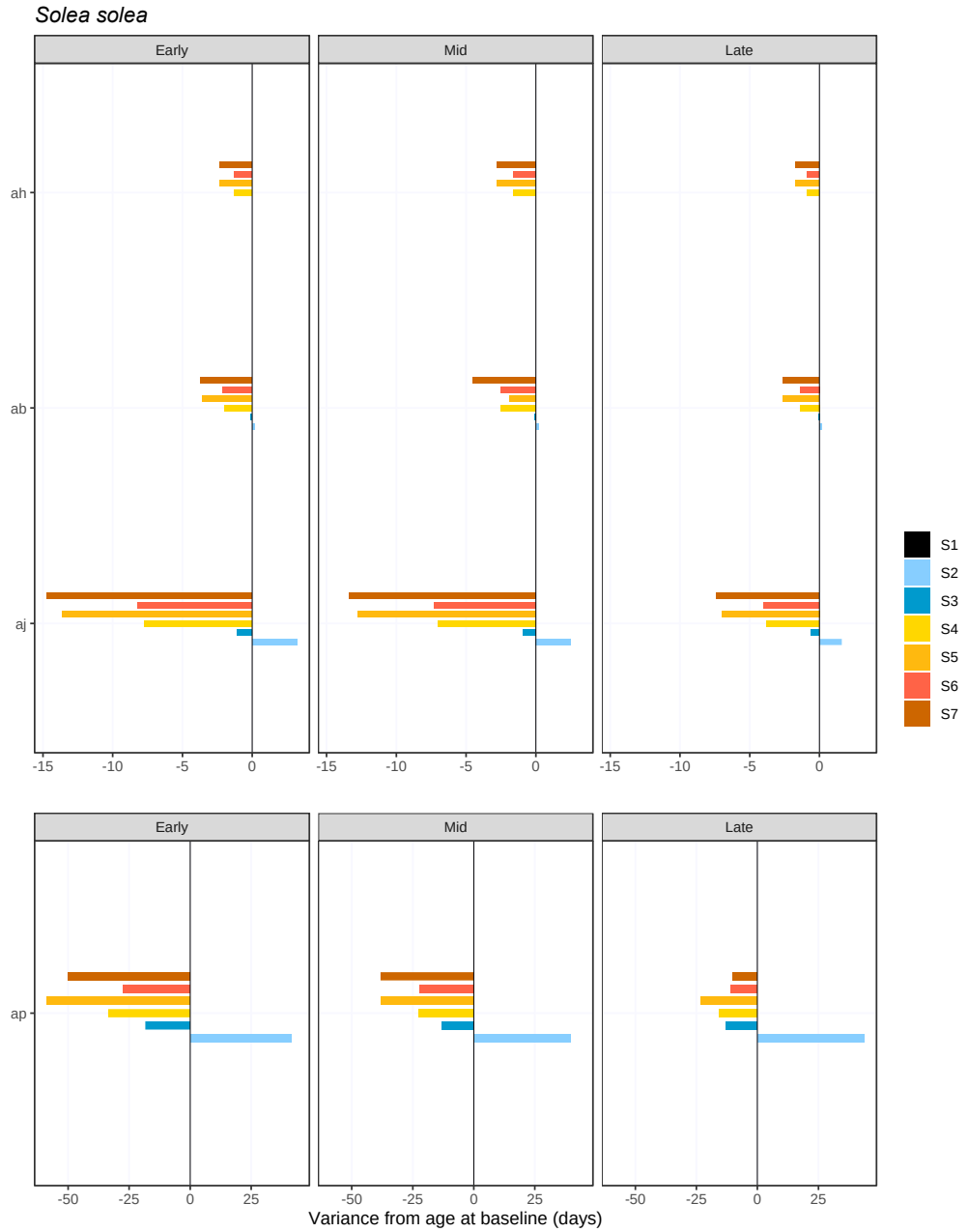


Figure 3. Time variance from baseline (S1, black line in figure) for age at hatching (ah), birth (ab, start of exogenous feeding), end of metamorphosis (aj), and puberty (ap) in *S. solea* individuals issued from early, mid and late spawning events and growing under the seven different scenarios (please see Table 1 for scenario descriptions).

For *S. solea*, the S5 (++TbX) and S7 (++T−X) scenarios hastened development the most, which is especially interesting for S7, where a larger temperature increase compensated for a 50% decrease in food availability compared with S6 (+T−X). Early spawned individuals (i.e., on 1 January) in scenario S7 exhibited a more pronounced difference for age at metamorphosis (aj, Figure 3) than those spawned mid and later in the year. Compared with the baseline scenario S1, a complete metamorphosis occurred 14.7 days earlier for early-spawned individuals and 13.4 and 7.4 days faster for those spawned mid and later on the year, respectively (Figure A5 in Appendix C). Similarly, the time to complete puberty

shortened the most in the S5 and S7 scenarios, with a maximum of 58.6 days difference between early-spawned larvae and baseline scenario ones in S5 individuals.

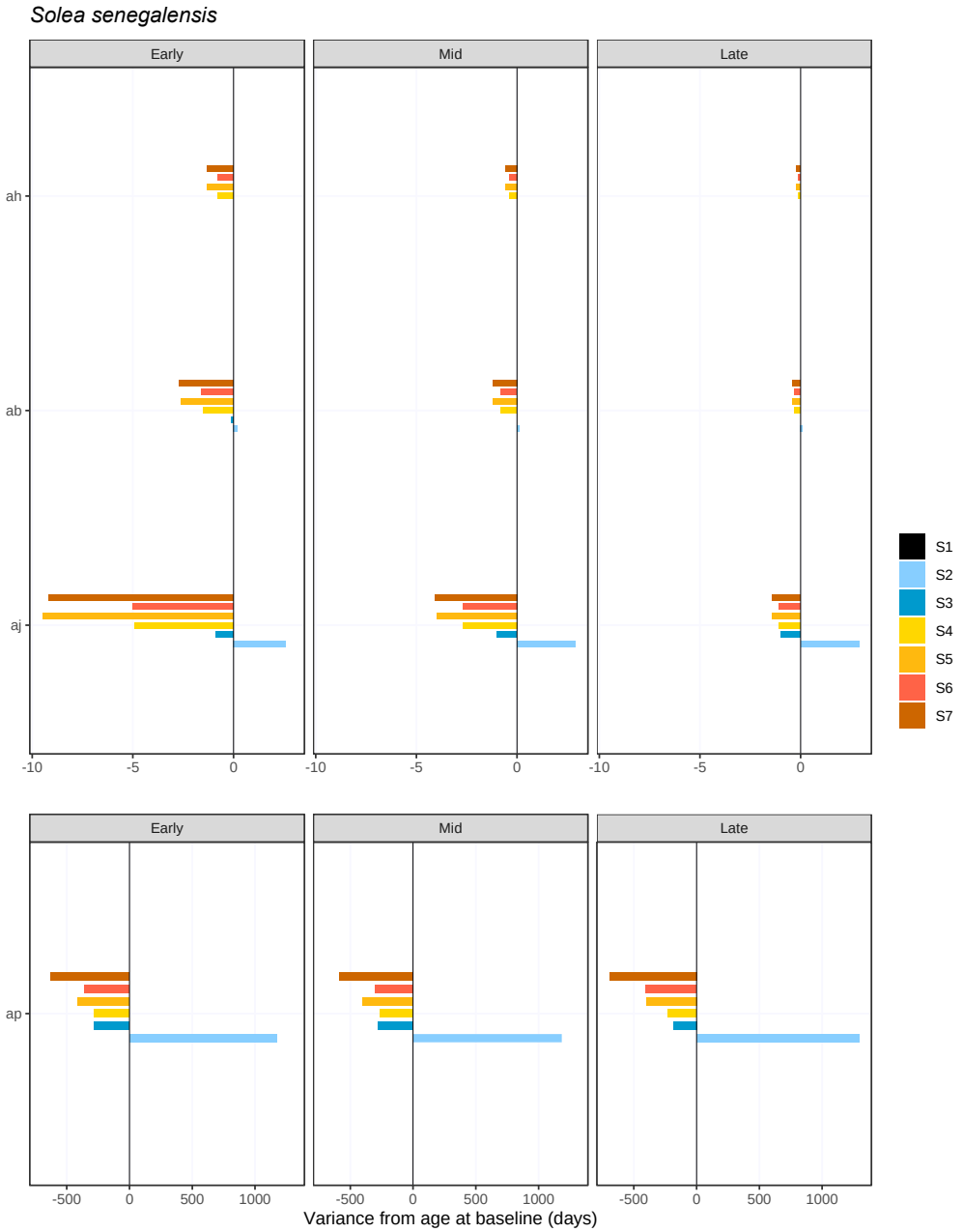


Figure 4. Time variance from baseline for age at hatching (ah), birth (ab, start of exogenous feeding), end of metamorphosis (aj), and puberty (ap) in *S. senegalensis* individuals issued from early, mid and late spawning events and growing under the seven different scenarios (please see Table 1 for scenario descriptions).

The differences in the stage duration until complete metamorphosis were less marked for *S. senegalensis*, which showed a maximum of 9.5 days difference between baseline and the S5 (++TbX) scenario for the early-spawned individuals, while the difference was less than a day and a half in late-spawned individuals (Figure 4, top).

Regarding age at puberty, late-spawned soles were generally a bit faster than mid and early-spawned fish in reaching puberty. The highest difference from baseline was obtained for *S. senegalensis* individuals issued from the last spawning event of the year (day 210, 1 August) and under the S7 (++T−X) scenario, where it would take up to 694 days less for individuals to reach puberty than individuals from its corresponding baseline scenario.

Changes in food availability and temperature impacted, to a lesser extent, the age at hatching and age at birth. In both species, a slight reduction in the age at birth was observed, notably for the scenarios involving an increase in temperature. In *S. senegalensis*, changes in the age of birth—the age at which exogenous feeding starts—were more evident for early-spawned individuals but always lower than 2.7 days, which was the maximum difference recorded for S7 (++T−X) scenario (early spawns). In *S. solea*, the highest time variance for age at birth was obtained in S7 individuals from the mid-spawn, which started exogenous feeding 4.5 days earlier than baseline individuals. The food availability did not alter the age at hatching or birth, which at this period are processes regulated by the amount of energy available in the egg yolk and yolk sac.

3.3.2. Food Availability Reduction Is Delaying Development and Thus Increasing the Stage Duration

For both species, age at metamorphosis and puberty were consistently higher in larvae from the S2 scenario (bT−X, Table 1), where food availability was reduced by 50% compared with the baseline and temperature was unaltered (S1: bTbX) (Figures 3 and 4). The increase in time for completing metamorphosis varied among spawning events, although, for both species, it was always less than three days compared with the baseline scenario (Figures 3 and 4). The age at puberty was notably delayed for both species: *S. solea* juveniles took, on average, 42 more days (compared with S1 juveniles) to complete maturation (Figure 3, bottom panel), whereas *S. senegalensis* juveniles needed over 1000 additional days to complete maturation (Figure 4, bottom, see also Table S1).

3.3.3. Larval and Juvenile Growth Rates

As a broad pattern, a rise in temperature increased growth rates in both species, and a decrease in food availability had the opposite effect, which was offset or even fully compensated when the two factors acted together (S6: +T−X, S7:++T−X). The effect depended on the time of spawning and the species (Figures 5 and 6, see also Figure A6 in Appendix C): for example, a temperature increase affected larval phases of early *S. solea* spawners more than late *S. solea* spawners (Figure 5b,c), but the decrease in food availability hit late spawners of this species harder (Figure 5a). Late spawners of *S. senegalensis* also exhibited higher sensitivity to decreased food availability than earlier batches (Figure 6a), but the responses to temperature increase were similar between batches, with relatively little effect within the first few months (Figure 6b,c).

Predicted growth rates (in length) varied according to the developmental stage (Figures A5 and A6), especially for *S. senegalensis* individuals. The growth rates in length declined with fish age and were highest for larvae stages—i.e., from birth to metamorphosis —ranging from 0.080–0.140 cm d^{-1} in *S. senegalensis* and 0.037–0.091 cm d^{-1} in *S. solea* larvae. For both species, the lowest growth rates were observed in individuals under the S2 (bT−X) scenario (0.08 and 0.037 cm d^{-1}, for early-spawned *S. senegalensis* and mid-spawned *S. solea*, respectively). In contrast, the maximum growth rate corresponded to late-spawned *S. senegalensis* (0.140 cm d^{-1}) and *S. solea* (0.091 cm d^{-1}) larvae under the S5 (++T-bX) scenario.

When comparing growth rates between the two species, *S. senegalensis* larvae showed, for all simulated scenarios, higher growth rates than *S. solea* larvae, which has a more homogeneous growth rate between larvae and juveniles, and as such, a less drastic difference in developmental stage growth rate than the Senegalese sole (Figure S1). Interestingly, the highest temperature increase (scenarios S5: ++T-bX and S7: ++T−X) affected, overall, the late spawners of both species more severely than earlier spawners, but in the opposite direction: while *S. solea* individuals grew at times slower than their temp-baseline counterparts, *S. senegalensis* individuals grew faster (Figures 5b,c and 6b,c).

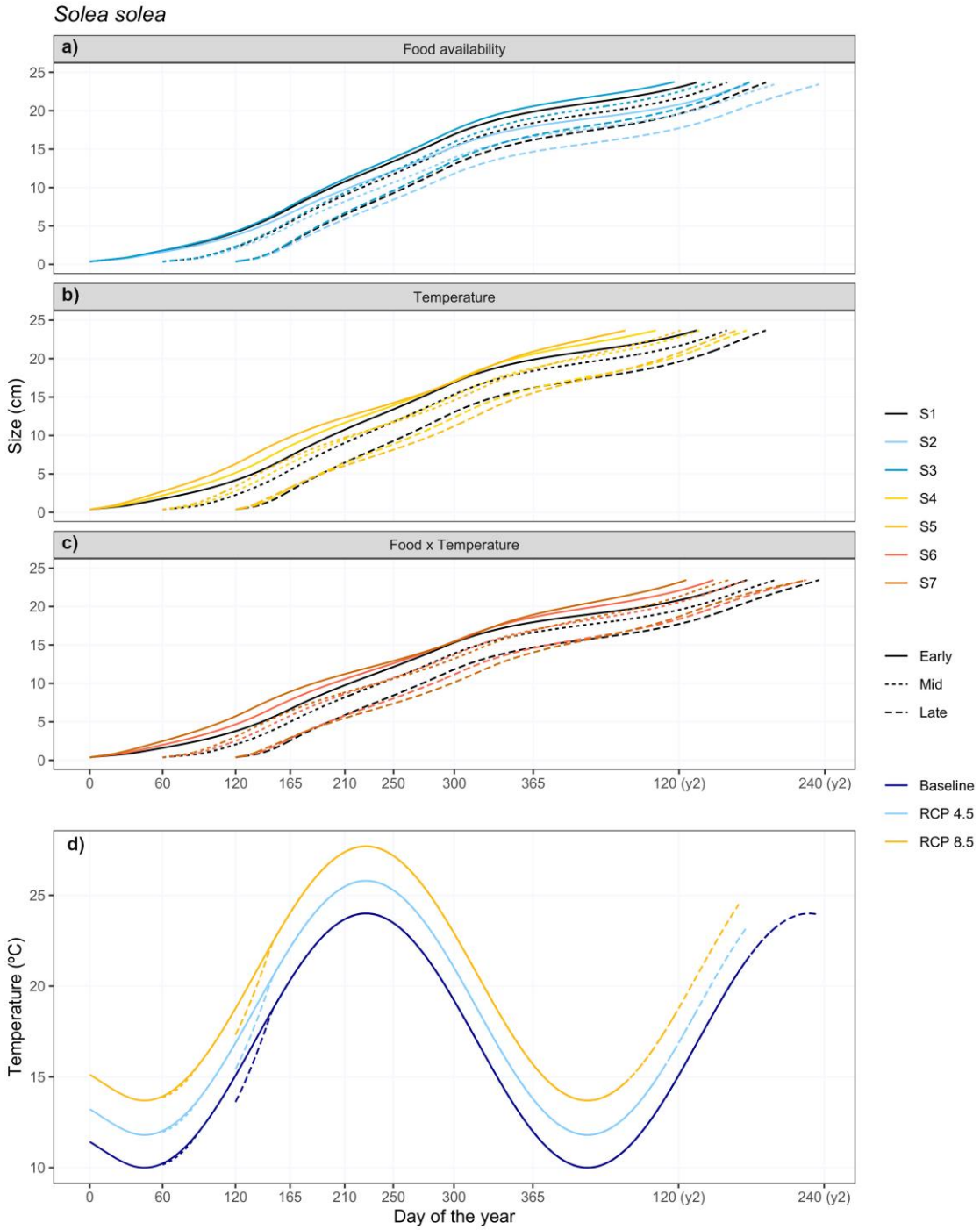


Figure 5. DEB model growth simulations for *S. solea* individuals spawned at three different times of the year (represented by full, dotted, and dashed lines) under baseline conditions (S1, black lines in panels a-c), and (**a**) magnitude changes of food (±50% X, S2 and S3. blue lines), (**b**) temperature rise scenarios (+1.8 °C and 3.7 °C, yellow lines) and (**c**) their combination (S6 and S7, orange lines). (**d**) Temperature during the simulation, representing the temperature experienced by the larvae and juveniles, i.e., it includes the gradual shift from coastal sea to estuary (see Methods for details). Please see Table 1 for the summary of scenario descriptions.

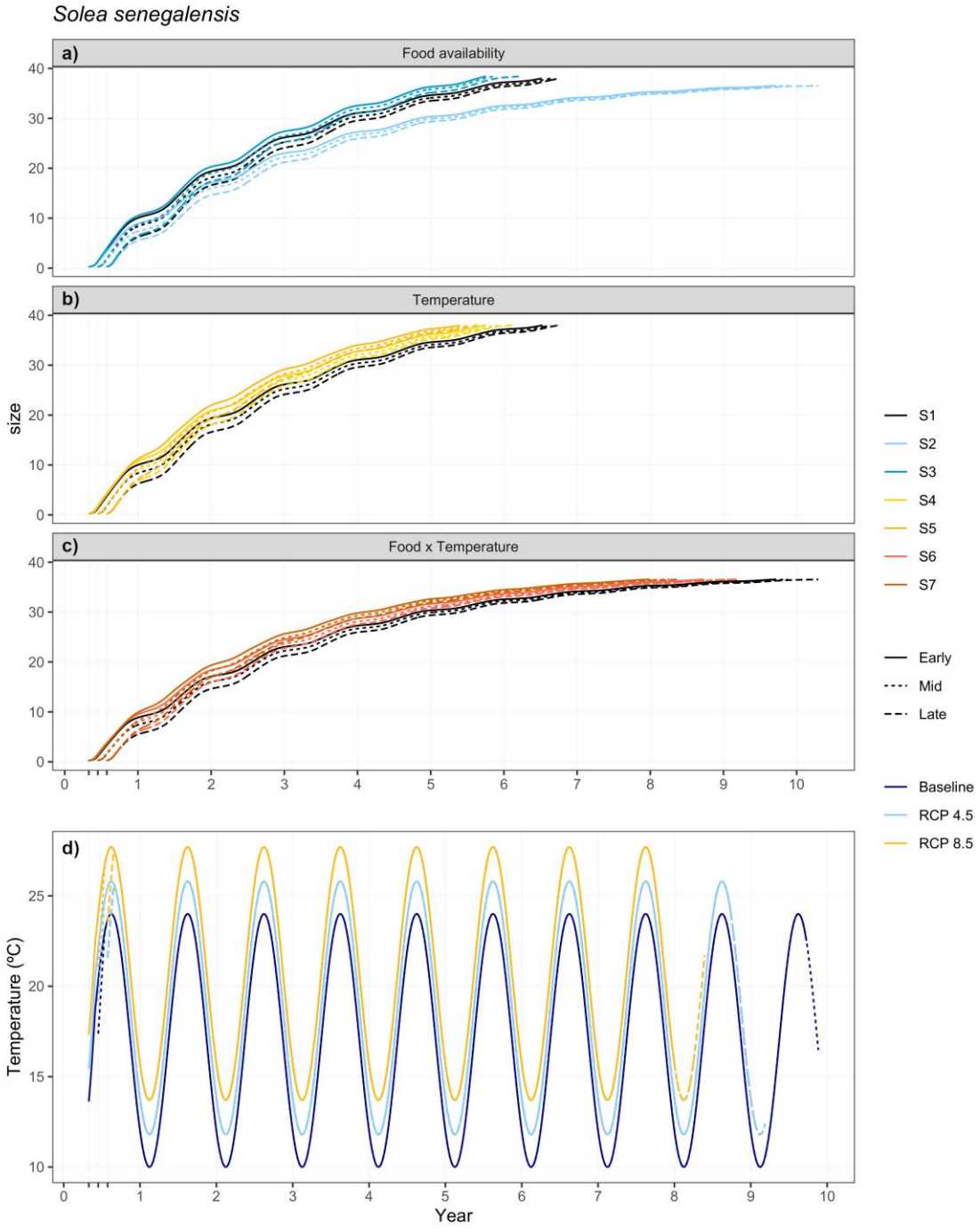


Figure 6. DEB model growth simulations for *S. senegalensis* individuals spawned at three different times of the year (represented by full, dotted, and dashed lines) under baseline conditions (S1, black lines in panels a-c), and (**a**) magnitude changes of food (±50% X, S2 and S3, blue lines), (**b**) temperature rise scenarios (+1.8 °C and 3.7 °C, yellow lines) and (**c**) their combination (S6 and S7, orange lines). (**d**) Temperature during the simulation, representing the temperature experienced by the larvae and juveniles, i.e., it includes the gradual shift from coastal sea to estuary (see Methods for details). Please see Table 1 for the summary of scenario descriptions.

4. Discussion

Studying the impact of CC-induced changes in food availability and temperature on the ontogenetic development of fish larvae seems necessary in the context of global change and biodiversity loss, coupled with the ongoing changes the planktonic communities have

faced for several decades [7]. Here, we used DEB models for forecasting and comparing fish early life-history traits of two commercially relevant species (*S. solea* and *S. senegalensis*) under seven distinct future CC scenarios. The direct comparison (simulating identical environmental conditions to forecast the responses of two distinct species) was possible after independently parameterizing and validating models with species-specific parameter sets. We will discuss (i) the assumptions and choices made while parameterizing models and designing the study, (ii) the main results of model parameterization, validation, and simulations, (iii) the implications of our results in the wider context of climate change, and (iv) further research.

4.1. Study Design—Assumptions and Choices

We have made several explicit assumptions and choices while designing the study. The process was motivated by literature and experience, but as the choices determine the scope and applicability of the results, we feel it is useful to discuss each of the major assumptions and choices.

All individuals are physiologically equal. To simplify the study design and results interpretation, all individuals of the same species are assumed to be physiologically equal, *i.e.*, they are described by the same set of (species-specific) parameters [20]. Clearly, this is not the case in nature, where much of the inter-individual variability stems precisely from physiological differences. When sufficient information is available and inter-individual variability is in focus, variability can be integrated into DEB models via one or more physiological parameters (e.g., [59,60]). However, our choice was motivated by the overall aim to focus on the role of the two environmental factors (temperature and food availability) in shaping observable responses in growth and maturation rates while excluding differences resulting from other factors (e.g., as was done in [38,54,55]).

Characterizing the hypothetical location. For the baseline conditions (temperature and food availability), we used a temperature year function representing a hypothetical location from the west coast of France and Portugal and have coupled this temperature function with constant food availability, represented by a scaled functional response of $f = 0.85$ for both species, which decreases during migration. The choice was, again, motivated by study focus and supporting literature. Even though the location temperature characteristics favor the growth and maturation of *S. solea* over *S. senegalensis*—a more subtropical species—the represented location does support both species [61–63] and might become more accommodating for *S. senegalensis* in the context of CC-induced temperature increase. Constant food availability—as applied in similar studies [38,54,57,64]—was preferred over some function of food availability because proxies generally used to construct such functions (e.g., chlorophyll a) vary irregularly between different years and micro-locations, as does water turbidity, hindering the design of a representative food function. However, the methods and models applied here could be used for a particular area, for which specific temperature and food density functions could be implemented, as was done in, e.g., [55,56].

Mother's nutritional status determines the egg size. Egg size and the availability of energy from the yolk are conditioned to the mother's status (i.e., see the maternal effect in [20,65]. Without information on the mother's status and in the context of constant food availability in simulated environments, eggs of a species were assumed to be of the same size throughout the simulation. Devauchelle et al. [66], however, reported smaller *S. solea* eggs with increasing temperature, implying that these eggs have a lower energy content. Because higher temperatures are usually associated with being later in the spawning season, this could imply energy limitations experienced by mothers later in the spawning season, which could be included in the model. Under the current setup, the models' predictions fail to illustrate the natural variability in individuals hatching with different energetic contents. However, should a need arise, it is possible to include variability in egg size—via the maternal effect and/or stochastic variability [59]—where the initial energy in an egg is adjusted to the temperature and/or spawning time and corresponds to a lower f (energy

limitation) experienced by the mother, followed by a higher *f* after settlement into estuaries, i.e., nutrient-rich environments.

Migration as a passive journey. We modeled the larval migration as passive transport lasting 30 days. During this period, we assumed larvae have a 25% lower *f* compared with that experienced by fish outside the migration period. In addition, larvae were gradually exposed to the temperature of the estuary as opposed to that of the sea. The duration of the migration period was assumed to be dependent on abiotic factors only (mainly sea currents) and therefore was the same for both studied species. The assumptions for the 'migration' were motivated by the literature suggesting mostly passive drift [3,5] and larvae reaching estuaries almost or completely metamorphosed [3,5,46,47]. In reality, the migration duration—as well as recruitment success in the estuaries—depends on multiple biotic and abiotic factors; and includes, to an extent, active swimming by larvae, which not only differs between individuals of different species but also between individuals of the same species, showing temporal and spatial variation (e.g., [3,5]). Duration of larval development—happening in parallel with the migration—is, in turn, also highly dependent on biotic and abiotic factors and can have a range of values up to 40 days (Table S1 in [3,53]; see also our results). Setting the migration duration as fixed 30 days in our simulations is a reasonable and approximative choice but can be modified if more precision is needed.

Food and temperature as the main drivers of CC-induced effects. In this work, we simulated the effects of food and temperature—two important environmental drivers—in sole metamorphosis success separately, but in nature, they are unlikely to operate independently. Furthermore, each (or both) of these factors might be further combined with the effects of ocean acidification and/or hypoxia [67]. Even though some preliminary work has been carried out on the effects of acidification on sole development [64], we have decided to focus on the better-documented and much better-studied effects of temperature and food availability. To elucidate better the effects of food availability, we simulated a theoretical increase in food availability (scenario S3), but research indicates that a lower scaled functional response *f* is much more likely than a higher one, as shown for anchovy with *f* values estimated mostly below 0.8 [55,56], so more focus is given to interpreting the food reduction scenarios. In addition to exploring the effects of food and temperature (scenarios S1–S5) separately, the two simulated scenarios combining the effects of temperature and food (S6: +T−X and S7:++T−X) capture situations where CC-induced temperature increase results in energy-depleted oceans, which seems quite likely [7].

Parametrization of the model using aquaculture data. Finally, a minor but valid point is that a lot of the data used for model parameterization (see Appendix B) is obtained from aquaculture, whereas the simulations focus on wild populations. Generally, individuals reared within aquaculture facilities are well fed and raised at higher temperatures, which enhances growth, and as a result, aquaculture soles grow and mature faster than wild individuals. Aquaculture of the Senegalese sole has managed to make fish reach puberty within 2–2.5 years when the individuals reach an average weight of 700–1000 g, while in the wild, the transition from juvenile to adult can take between 4 to 7 years, depending on the location [30]. Regardless of using aquaculture data for the model parameterization, our models were able to reproduce these characteristics with an initial spawning between 5 and 7 years of age (Figure 6b). In fact, one might argue that it is precisely *because* aquaculture data were available, with monitored and recorded temperature and feeding conditions—which could then explicitly be taken into account—that we were able to parameterize the model for both species with such success (see Appendix B for model fit to data from both aquaculture and the wild).

4.2. Implications of the Main Results

4.2.1. Model Parameterization and Validation

Generally, parameter sets for both species produce good fits to data used for model parameterization (Appendix B) as well as good fits to validation data (Figures 1 and 2). As expected for closely related species belonging to the same genus, parameter values

are similar between the two species, with some exceptions (see Results, Table 2), which might have been influenced by the availability of data used for model parameterization. Namely, the relative abundance of larval data used for *S. solea* parameterization might have influenced a somewhat higher value for the parameter T_A, implying a higher temperature sensitivity. We discuss this in more detail later in the discussion.

Model validation was carried out on experimental laboratory data. Finding relevant data for validation is often a challenge, particularly when evaluating the effects of multiple variables. Here, the experimental data imply a substantial difference between the expected and estimated food availability (f): while the experimental protocols aimed for *ad libitum* food (analogous to $f = 1$), estimates for high food treatments were much lower for both species (f ranging from 0.10 to 0.45). The relatively low estimates for f might result from insufficiently nutritious food items provided under an *ad libitum* feeding regime —either due to quantity or quality (variety) of food— as suggested for *S. solea* by Mounier et al. [38] and partially addressed for *S. senegalensis* by Sardi et al. [44], or due to inappropriate (too small) rearing containers. Feed not matching the realistic needs of commercial fish has already been demonstrated for another well-studied species (bluefin tuna [68]).

4.2.2. Larval and Juvenile Growth Are Affected by Temperature and Food Availability

As a general pattern, growth rates were positively affected by an increase in both temperature and food availability (Figure A6), and ultimate size (implied by the growth curve) was affected by food availability (Figures 5 and 6). These results are in line with simulations of similar type [38,54,57] and have much to do with the model setup, but also do reflect what we can observe in nature.

Growth retardation over colder months (winter) was much more evident for *S. senegalensis*, the species for which simulations (lasting until puberty was attained) also lasted substantially longer: up to 10 years, compared with those for *S. solea*, lasting up to 2.5 years. *S. senegalensis* also had a more pronounced positive response to the more drastic temperature increase (+3.7 °C), whereas juveniles of *S. solea* that were spawned late even exhibited a negative response compared with the baseline (see Figure 5b). The patterns can most likely be explained by the different ecology of these species—*S. senegalensis* generally prefers warmer waters (but see [69])—which was accounted for in the model in the form of critical high and low temperatures (Table 2). Research shows that raising larvae at higher temperatures accelerates their growth rate (e.g., [70]), but the ultimate size decreases with increasing temperature—also known as the temperature-size rule (TSR [71]). Consequently, at higher temperatures, individuals do not necessarily attain their max size, resulting in smaller fish body sizes [72]. The reason may be directly related to the feeding rate, which also increases with temperature (i.e., food supplies will likely become limited at higher temperatures, reducing the ultimate size [20]), or to oxygen limitation, i.e., oxygen availability as the critical factor limiting growth becomes especially relevant at higher temperatures [73–75]. Ultimate size (of adults) could be relevant for recruitment: larger body size is (with high variability) positively correlated to fecundity [76,77], which, in turn, has been linked to higher recruitment variability [78]. However, the mechanisms behind the TSR in ectotherms are still an issue of debate in the scientific community [79] and are out of the scope of this study.

Size has been hypothesized to alter survivorship in several ways. Predation and "the bigger and faster relationship" depend on individuals' size; as such, faster growth and larger body size are assumed to increase the survival probability of fish (but see [80,81]). In flatfish, the size at settlement—which has also been identified as a proxy for juveniles' survival—is also influenced by the pelagic larvae duration (PLD) [53], which is, in turn, affected by the same abiotic factors (see next section). Larger sizes at settlement may offer some survival advantages, but small individuals settling in warmer conditions may grow faster after settlement and quickly reach equivalent sizes to fish settling in cooler conditions [82]. When studying the size composition of fish stock at any given time, it is important to keep in mind that the observed size can be a result of many complex

interactions, as shown by our simulations. Even while assuming all individuals of the same species are physiologically identical and thus excluding inter-individual variability, our simulations predict that, for example, in January of the second year, the hypothetical nursing grounds will contain *S. solea* juveniles ranging from 15–20 cm total length, and *S. senegalensis* juveniles ranging from 5–10 cm total length. The size range, in our case, is a result of (i) age: *S. solea* individuals are between 8 and 12 months old, and *S. senegalensis* juveniles are between 5 and 8 months old; (ii) temperature: all of the *S. solea* individuals experienced peak high temperatures of the summer (June–August), whereas some *S. senegalensis* were spawned at the end of the warm season and consequently experienced only several months of winter temperatures, and (iii) food: some simulations included a higher, and some a lower food availability. In nature, the inter-individual variability will be affected by even more factors.

4.2.3. Developmental Rates Are Affected by Temperature and Food Availability

The simulation results demonstrate that both temperature and food availability affect development rates. A temperature rise reduced the time required for the occurrence of exogenous feeding and metamorphosis in pre-metamorphic larvae. The decrease in food availability, however, had a more pronounced effect on the period required for juveniles to reach puberty, especially for *S. senegalensis*. When the simulations combined temperature rise with food reduction (S6 and S7), the stage duration was slightly prolonged, indicating that the reduction of energy availability partially counterbalanced the acceleration effect of temperature rise. These results directly affect the population renewal, and they also imply—especially for later batches—more prolonged use of the nursery, where fish are more exposed to anthropogenic pressures, including exposure to pollutants, fishing, and heatwaves.

Metamorphosis is an energy-demanding process; as such, a food reduction simulated in scenario S2 delays the onset of metamorphosis, and larvae reach metamorphosis at an older age. However, the reduction in food availability did not delay the onset of metamorphosis in both species when combined with higher temperatures (S6 and S7). This counterintuitive result might indicate the need to include survival predictions and, more explicitly, model the physiological stress potentially experienced at higher temperatures [69]. Specifically, the survival probability of larvae might decrease if hastened growth (and development) is not coupled with abundant food [80,81], which was not the case in scenarios where a temperature increase was coupled with food reduction (S6, S7). In our results, the lesser effect of changes in food availability—particularly between scenarios S2, S6, and S7—on the early stages of larvae development (hatching and birth = mouth opening), as well as on the age to complete metamorphosis, reflects the influence of running simulations using the same initial reserve energy. Namely, the availability of energy from the yolk was assumed to be the same within the models because all eggs of the same species were assumed to be of the same size. In nature, larvae issued from large eggs with a large yolk sac have a higher energy supply (yolk) when they hatch [83] and thus have a greater chance of surviving than those with a small yolk sac, especially if food is scarce. As a result, individuals' variability in the energy reserve would potentially result in differences in the stage duration between birth and the end of metamorphosis. From a simulation point of view, this could be solved by comparing larvae growth using different initial reserve energy content values, but detailed information is needed to compile a realistic range of values.

4.3. Context: Phenology, Phenological Adaptations, and Potential Mismatches

Soles are batch spawners, with the timing of spawning induced by temperature: for *S. solea*, the optimal temperature for spawning ranges from 8 °C to 12 °C, whereas for *S. senegalensis*, the water temperature should be between 15 °C and 20 °C [45]. We took this into account by simulating three spawning events (early-middle-late) for each species, corresponding to early January, early March, and early May for *S. solea* and for *S. senegalensis* early May, mid-June, and early August [45]. We did not evaluate/simulate

the effect of temperature on the timing of spawning, but the observed variations in the intensity of the effect did depend on the spawning batch, with the fish spawning the latest being the most affected (Figures 3–6). For *S. solea*, the effects were negative for the highest simulated temperature, which reached the thermal tolerance for this species when larvae hatched in May. For *S. senegalensis*, the simulated temperature rise had a positive effect, but the food limitation drastically prolonged the maturation process. This was especially evident in late spawners who, possibly due to water temperatures decreasing soon after spawning (occurring in August), underwent growth and development retardation as *low* temperatures reached their thermal tolerance. Indeed, the times until yolk absorption, metamorphosis, and PLD of fish larvae are all negatively correlated with temperature [82]. All temperature rise simulations (S4–S7) advanced the onset and reduced the stage duration of metamorphosis in both species, and because mortality is generally very high during the larval phase, faster growth and shorter PLD at higher temperatures could positively affect larval survivorship [82]. However, should larvae metamorphosize entirely before reaching the estuarine nursery areas, they will be vulnerable to predation in an environment low in prey and will need to spend their energy trying to reach the estuaries, which will probably negatively impact their survival probability, as also suggested in Pepin et al. [84]. In that context, it might be advantageous for both species to shift spawning earlier in the season, to avoid high temperatures (*S. solea*) or lower temperatures with low food availability (*S. senegalensis*).

Organisms that are dependent on temperature to stimulate physiological development and larval release—such as *S. solea* and *S. senegalensis*—have significantly moved forward in their seasonal cycle in response to temperature [10]. Further, another study demonstrated that globally, spring phenologies of all marine species have advanced by 4.4 $\pm$ 1.1 days per decade since the mid–20th century [11]. Phenological adaptations also constitute, for fish, an important mechanism to tackle the changing climate [12]. Indeed, a study that estimated the peak spawning time in seven different subpopulations of sole from 1970–2010 demonstrated that at least four of the seven studied stocks of *S. solea* showed a significant long-term trend toward earlier spawning at a rate of 1.5 weeks per decade [13].

The impacts of temperature-induced changes in sole phenology are hard to predict and demonstrate. Even though spawning earlier might mitigate a mismatch between metamorphosis and arrival into nurseries, temperature-driven changes in phenology could cause a mismatch between different trophic levels and negatively affect recruitment by directly increasing mortality and extending the metamorphic period. Climate change is causing variations in the peak and seasonality of primary production in the oceans [85], pointing to a reduction of food availability for pelagic larval stages. Although many pelagic organisms are responding to water warming, it is, however, the intensity of the response that varies. The onset of metamorphosis requires larvae to acquire a competent size [53], and if the conditions are not favorable for growth, metamorphosis takes longer and renders larvae vulnerable to predation [82]. This was observed in S2 simulations, which accounted for the highest median duration for metamorphosis in *S. solea* (30 days) and *S. senegalensis* (~27 days). The scenario S2 (bT−X) can well represent the phenological adaptation of fish spawning earlier in the season (to experience lower temperatures in the future, akin to current temperatures at spawning) but, due to a phenological mismatch with the (rest of the) planktonic community, experience a lower food availability.

4.4. Further Research

4.4.1. Temperature Tolerance Shifts during Ontogenesis—Parametrization of T_A

Changes in thermal tolerance along the life cycle imply that different developmental stages might react differently to temperature fluctuations. A narrow tolerance range suggests that the individual is exposed to small temperature changes, and this, in turn, is usually linked to a relatively high T_A value. In DEB models, the Arrhenius temperature parameter (T_A) describes how metabolic rates are affected by temperature. The value of the T_A is the resulting slope after plotting the log of any metabolic rate against the

inverse absolute temperature [20]. The T_A is typically low (~6 kK) for species that experience extreme temperature changes, like in the intertidal zone, and higher (~12 kK) for species that experience temperature changes in a narrower range as would be, for instance, pelagic species [20].

One of the challenges we encountered while parametrizing the *Solea* spp. models was related to the T_A parameterization, which seemed to be different for larvae vs. adult individuals. More precisely, data for developmental rates (hatching and birth) and growth in larvae suggest a higher slope of ~10–12 kK, while data describing juvenile and/or adult growth rates result in a slope of ~7000 K. As we could not source sufficiently detailed data on various metabolic rates for larvae, juveniles, and adults, we opted for a constant (average) T_A value estimated by DEBtool parameter estimation routines (Table 2), which results in acceptable predictions for both larvae and later life stages (Appendix B). Having said that, we did put a stronger emphasis on larval data (as early life stages are the focus of this study), either by including more data for early life stages during parameter estimation (*S. solea*) and/or by giving higher 'weights' to early life-stage data during parameter estimation (both species). The estimated value of T_A is around 8000 K for *S. solea* and 6500 K for *S. senegalensis* (Table 2), compared with T_A of around 4500 K for *S. solea* in work by Mounier et al. [38]. As a result, our model predictions for *S. solea* match better data for early life stages, which is the opposite situation than in work by Mounier et al. [38], who focused on later life stages, while sacrificing the fits on early life stages. For *S. senegalensis*, the T_A value might have been higher if more larval development data had been included, but the only other available dataset [86] did not match other data for the species and was therefore excluded.

In general, it is assumed that T_A, like most other parameters, remains constant throughout the ontogeny of an individual and is species-specific [20]. The same holds for other parameters (T_{AL}, T_{AH}, T_L, T_H) that together define the optimal thermal niche, critical high and low temperature, and physiological responses to temperature shifts. However, evidence suggests that thermal tolerance shifts during the life cycle of fish species [87] and that the optimum temperature for growth decreases with the increasing body size of juveniles and adults [14]—a difference in thermal responses of life stages suggested also by our analysis. Thermal tolerance range might differ between fish larvae and adults due to respiration capacity varying between developmental stages [88]. In that sense, the changes in thermal tolerance during the life cycle correspond to the development of aerobic capacities and cardiorespiratory organs. Specifically, tolerance ranges are hypothesized to widen from embryo to larval and adult stages. During reproduction (spawning stage), tolerance ranges may narrow again due to a net decrease in the aerobic capacity associated with additional energy and, thus, O2 demand for gamete production and biomass [87]. This hypothesis supports the common observation that shows larvae have the highest sensitivity to environmental stressors [82]. It would also explain the differences observed while calibrating the T_A parameter using larval or juvenile/adult data. This could be included as a simple model extension, akin to the modification enabling several parameters to change their value throughout ontogeny in the abj-type model, [36,37] also applied here. The thermal response might also be population specific, where (sub)tropical populations tolerate higher temperatures which cause stress in colder-water populations of the same species [69,89]. However, for a meaningful model extension, detailed experiments and data are needed, particularly data on metabolic rates (e.g., development, growth, ingestion, respiration) for all life stages of both species under controlled feeding regimes and several different temperatures. Such data were not available at the time of the study (so constant T_A was assumed as a good approximation) but developing life stage- or population-specific temperature responses could be a valuable study direction, especially in the context of climate perturbations, including heat waves.

4.4.2. Survival Calculations Made Explicit

We have focused on energetic pathways and consequences of environmental perturbations (temperature increase, food availability increase or decrease) on the growth and development of sole individuals. This is an appropriate tool for studying fish recruitment, as developmental changes require energy and allocation, and the critical size for switching between life stages can be quantitatively linked to DEB parameters and modeled processes [90]. However, larvae survival modeling simulations should also be considered for forecasting recruitment. DEB (individual) models can easily be coupled to a population model that includes survival, as was done, e.g., for the early life stages of bluefin tuna [91]. As another example based on soles, Van De Wolfshaar and collaborators [92] estimated the number of viable *S. solea* larvae surviving the phase from the egg until settlement in a nursery by calculating the survival of post-settlement juveniles for a particular set of estuaries, years, and climate scenarios using the length-based mortality rate function. The authors based their calculations on temperature-dependent mortality losses [92]. Because size determines mortality rate and early arrival is associated with low growth rates, early arrivals stay small for a longer period than late arrivals, and post-settlement survival of late arrivals is, therefore, higher than for early arrivals. We believe that by coupling the proposed modeling framework to a larval dispersion model, as in [92,93], we could provide detailed information on recruitment success for specific locations/nursery grounds.

5. Conclusions

Given the fast pace of change in the ocean environment due to climate change and pollution, it is likely that the status of the future soles will not be improved. The rapid development of fish larvae in warmer waters requires highly nutritive and available food, but warmer oceans—due to stratification and a change in predominant plankton communities—might exhibit long and inefficient food webs with poor nutritional quality [7]. This will impact the food availability of mothers, larvae, and juveniles. As a result, we could anticipate two scenarios, one with smaller egg size and another with larger but fewer eggs, larvae from which will again face energy-impoverished environments. These scenarios logically denote a more extended period to reach metamorphosis and, thus, longer PLD and a reduction in survival and recruitment, respectively.

Modeling tools are necessary and practical for predicting the effects of climate change on fish recruitment. The DEB models calibrated and validated here showed potential, particularly by fitting the data very well. When confronting the model predictions to the experimental data used for validation, where feeding frequency is used as a food availability proxy, we noticed that fish were not fed until satiation, suggesting that the feeding regime was potentially insufficient in nutrition and quantity. This result points to the need to adjust and improve experimental larvae-rearing protocols, particularly regarding providing enough energy without compromising the larvae's health and rearing conditions.

Regarding timing for reaching a developmental stage, the effects of temperature rise seemed to counterbalance the effect of reduced food availability. Our results indicate the critical effect of temperature rise on the phenological cycles of both species, mainly by advancing the onset and the completion of metamorphosis. The growth simulations in both species indicate shorter pelagic stages responding to increased temperatures. However, changes in the PLD, which are *a priori* beneficial for larvae survival, when accompanied by a potential mismatch between hatching and the zooplankton cycle timing, result in more extended periods for maturation and smaller ultimate size. In that regard, the combined temperature-rise and food-reduction conditions simulated in scenarios 6 and 7 strongly affected the maturation age of *S. senegalensis*, which was significantly prolonged, notably for the latest batches, and would result in prolonged use of the nursery areas. This result might have important consequences in population renewal as it will take longer for the cohort to reach maturity and spawn new eggs. Additionally, we believe that coupling the proposed modeling framework to a larval dispersion model, like in [93], would provide detailed information on recruitment success for specific locations/nursery grounds.

To get a more holistic (and realistic) conclusion on the subject, it is necessary to include potential temperature-induced damage and mortality in the model, which might change between different life stages and/or populations [69,89]. Without including these potential negative effects, the overall conclusion is that temperature rise reduces the pelagic larvae' duration, potentially increasing the survival rates of larvae and, thus, recruitment. Additionally, survival should be explicitly included in the models, accounting for physiological temperature tolerance ranges, as well as size and habitat-linked mortality.

Finally, the survival and ontogeny of fish larvae may directly influence the future abundance of adult fish stocks. The latter has been, and still is, the most important reason for studying ichthyoplankton, as most processes determining the recruitment strength and the spatial distribution of fish populations occur during the planktonic stage of fishes, resulting in critical interannual fluctuations in fish stock biomasses. While questions on recruitment success and larvae survival were not our focus and thus remain unanswered, understanding the physiological mechanisms behind temperature increase and food limitation via DEB models provides a powerful tool for studying the role of early-life history traits on population renewal under climate change.

Author Contributions: Conceptualization, A.E.S., N.M. and J.M.M.; methodology, A.E.S., N.M. and J.M.M.; software, N.M. and J.M.M.; validation, A.E.S. and N.M.; formal analysis, A.E.S. and N.M.; investigation, A.E.S., J.M.M. and N.M.; data curation, A.E.S., J.M.M., L.O., M.M. and N.M.; writing—original draft preparation, A.E.S., N.M. and J.M.M.; writing—review and editing, M.-L.B., X.C. and M.M.; visualization, A.E.S. and N.M.; supervision, M.-L.B., X.C., M.M. and N.M.; project administration, A.E.S. All authors have read and agreed to the published version of the manuscript.

Funding: J.M.M. was supported by the Portuguese Foundation for Science and Technology (FCT), project FISHBUDGET—Effects of climate change on marine fish energy budgets (PTDC/BIA-BMA/28630/2017). N.M. was supported by the Croatian Science Foundation (HRZZ), project AqADAPT—Adapting Marine Finfish Aquaculture to a Changing Climate (IP-2018-01-3150).

Institutional Review Board Statement: All procedures for validation data were authorized by the Bioethics and Animal Welfare Committee of IFAPA as also by the Research and High Education French Ministry who evaluated and approved all animal experimentations within the project "Flatfish adaptation to temperature, feeding and pollution stress" led by Marie-Laure Bégout from Ifremer under the number reference APAFIS #38190-202208082103879.

Data Availability Statement: All data needed to evaluate the conclusions in the paper are present in the paper, the Appendices, and/or the publicly available Add-my-Pet collection (http://www.bio.vu.nl/thb/deb/deblab/add_my_pet/species_list.html (accessed on 1 December 2022)). Additional data related to this paper can be requested from the authors.

Acknowledgments: The authors would like to thank Florence Mounier for her helpful comments during the conceptualization and study design. The authors thank all the FISHBUDGET team for *S. senegalensis* data used in the parameter estimation.

Conflicts of Interest: The authors declare no conflict of interest.

Appendix A

Appendix A.1. Dynamic Energy Budget Model (DEB) Theory and DEB Models

In the Dynamic Energy Budget (DEB) theory [18,20,21], the focus is on energy—and mass—pathways in a (dynamic) environment, i.e., on energy and nutrient acquisition and subsequent utilization by an individual throughout its life cycle. In a DEB model, an individual is most often described and modeled by four state variables—energy reserve (E), structural volume (V), maturity (E_H), reproduction buffer (E_R)—and their interactions with the environment (mostly characterized by food and temperature) (Table A1). Energy and nutrients are assimilated from ingested food ($\dot{p}_A$) into reserves, which serve as a buffer in an environment with fluctuating food availability. Then, they are mobilized from reserves ($\dot{p}_C$) to fuel all biological functions: a constant portion of the energy (kappa, κ) is used for maintenance ($\dot{p}_M$) and growth ($\dot{p}_G$) of structural volume; maintenance has

priority over growth. The remaining energy $(1 - \kappa)$ is used for maturity—the cumulative energy invested in development or to become more complex (i.e., developing new organs, installing regulation systems; chapter 2 in [20]). Analogous with priority rules in the kappa-branch, the energy allocation for maturity maintenance ($\dot{p}_J$) has priority over increasing the maturity level for juveniles ($\dot{p}_R$ if $E_H < E_H^p$), *i.e.*, over-investing into reproduction for adults ($\dot{p}_R$ if $E_H = E_H^p$) (Table 1).

Table A1. State variables and main processes of the Dynamic Energy Budget (DEB) abj-model, which includes a change in parameter values between birth and metamorphosis.

State Variable	**Symbol (Units)**	**Dynamics**
Reserve energy	E (J)	$\frac{d}{dt}E = \dot{p_A} - \dot{p_C}$
Structural body volume	V (cm^3)	$\frac{d}{dt}V = \frac{\dot{p_G}}{[E_G]}$
Energy invested into maturation	E_H (J)	$\frac{d}{dt}E_H = \dot{p_R}(E_H < E_H^p)$
Energy invested into reproduction	E_R (J)	$\frac{d}{dt}E_R = \dot{p_R}\left(E_H = E_H^p\right)$
Process	**Energy Flux** ($J \cdot d^{-1}$)	
Assimilation:	$\dot{p_A} = \{\dot{p}_{Am}\} s_M f V^{2/3}\left(E_H \geq E_H^b\right)$	
Mobilization:	$\dot{p_C} = E\frac{[E_G]V^{2/3} + \dot{p}_S}{[E_G]V + \kappa E}$	
Somatic maintenance:	$\dot{p}_S = [\dot{p}_M]V$	
Maturity maintenance:	$\dot{p}_J = \dot{k}_J E_H^p$	
Growth:	$\dot{p}_G = \kappa \dot{p}_C - \dot{p}_S$	
Maturation/Reproduction:	$\dot{p}_R = (1 - \kappa)\dot{p}_C - \dot{p}_J$	

A DEB model quantifies the metabolic dynamics of an individual organism during its entire life cycle, mathematically describing the different processes of individual metabolism from the start of its development until its death. In DEB terms, the life cycle of an individual consists of an embryo, a juvenile, and an adult stage; transitions into stages occur when maturity level (E_H) reaches a certain threshold. Birth (maturity level E_H^b) marks a transition from embryo (does not feed or reproduce) to juvenile (feeds but does not invest energy into reproduction). Transitioning into adulthood is termed puberty (maturity level E_H^p) and is characterized by a switch in energy allocation from maturation into reproduction. Juveniles and adults assimilate energy from food, whereas embryos depend entirely on their reserve. In the standard (simplest) DEB model, all parameter values are constant from birth until death, but other typified DEB models exist [37]. The abj-typified model, applied here, is a 1-parameter extension of the standard DEB model. The additional parameter is the maturity level at metamorphosis (E_H^j), marking a life event within the juvenile stage, at which all parameters reach their final (constant) value [36]. The parameters affected in the abj-model ($\{\dot{p}_{Am}\}$ and $\dot{v}$) are linked to assimilation and mobilization. They are assumed to start at a smaller value at birth and then increase their value, i.e., 'accelerate' until metamorphosis. The change in a parameter value is modeled via the acceleration factor s_M, which is the ratio of the current length and length at birth. The s_M multiplies the initial parameter value (value at birth) and reaches its maximum and final value at the end of metamorphosis.

In total, we follow the soles through five life stages, with transitions between them marked by four corresponding maturity thresholds: hatching (maturity level E_H^h) marks the end of the egg stage, birth (E_H^b) marks the start of feeding and metabolic acceleration, metamorphosis (E_H^b) marks the end of metabolic acceleration and of physical metamorphosis, and puberty (E_H^p) marks the end of maturation and start of allocation to reproduction. Note that the main DEB-life stages (embryo, juvenile, adult) are still adhered to. Within the embryo stage (before mouth opening), we have an egg and an early larval stage. Within the juvenile stage, there are a larval stage (post-mouth opening and prior to complete metamorphosis) and a post-larval stage (after metamorphosis). The adult stage follows

the juvenile stage after puberty is reached. Isomorphy is assumed prior to birth and post-metamorphosis.

Throughout their life cycle, the soles, like many other species with metabolic acceleration and metamorphosis, change their shape and metabolism. To convert the structural length (L, predicted by the model) into physical length (Lw), we used a gradual change in shape calculated as:

$$\text{shape_vector} = \delta_{Me} + (\text{L} - \text{L}_\text{h})./(\text{L}_\text{j} - \text{L}_\text{h}) \times (\delta_M - \delta_{Me});$$

where δ_{Me} and δ_M are shape coefficient of larvae and adults (respectively), L_h structural length at hatching, and L_j structural length at metamorphosis. The formula was adapted from the *S. solea* AmP entry (2015, by F. Mounier).

Appendix A.2. Effect of Temperature on Rates, Arrhenius Temperature

Water temperature will strongly influence the energy budget and biology of ectothermic organisms such as fish. DEB theory argues that changes in temperature equally affect all metabolic rates (see Section 1.2 in [20]). The correction for the effect of temperature is done using the Arrhenius equation (from Equation (1.2) in [20]) within the optimum thermal niche ($C_T^{(1)}$ in Table A2), and is extended to a 5-parameter correction for a situation where temperature extremes are more likely ($C_T^{(5)}$ in Table S1.2, see also [34]). The full temperature correction function is available as a pre-coded function tempcorr.m in the freely available MATLAB package DEBtool_M [35], which was also used for parameter estimation.

Table A2. Temperature correction, coded as DEBtool function tempcorr.m. Parameters are as follows: T_ref—reference temperature, T_A—Arrhenius temperature, T_AL—low Arrhenius temperature, T_L—critical low temperature, T_AH—high Arrhenius temperature, T_H—critical high temperature.

Temperature Correction	Equation	Comments
1-parameter correction	$C_T^{(1)} = s_A = \exp\left(\frac{T_A}{T_{ref}} - \frac{T_A}{T}\right)$	Optimal temperature niche
5-parameter correction	$C_T^{(5)} = C_T^{(1)}\left(s_L^{ratio} + s_H^{ratio}\right)$, with	Complete temperature niche (optimal and critical temp)
	$s_L^{ratio} = \frac{1+\exp\left(\frac{T_{AL}}{T_{ref}} - \frac{T_{AL}}{T_L}\right)}{1+\exp\left(\frac{T_{AL}}{T} - \frac{T_{AL}}{T_L}\right)}$ and	applied for $\text{T} < T_{ref}$
	$s_H^{ratio} = \frac{1+\exp\left(\frac{T_{AH}}{T_H} - \frac{T_{AH}}{T_{ref}}\right)}{1+\exp\left(\frac{T_{AH}}{T_H} - \frac{T_{AH}}{T}\right)}$	applied for $\text{T} > T_{ref}$

Appendix B. *Solea* spp. Add-My-Pet Model Parameterization

Appendix B.1. Solea Solea

The model for *S. solea* was parameterized using the data listed in Table A4 and Figures A1 and A2. Model parameters are listed in Table A3. Initial parameter values and the model structure were based on the *S. solea* entry in the Add-my-Pet database (AmP, Teal, 2015, AmP Solea solea, version 2015/08/28) and the model published by Mounier et al. [38]. We included additional data on larval growth and re-estimated model parameters. COMPLETE = 3.3; MRE = 0.102; SMAE = 0.109; SMSE = 0.024. The parameter set, data, and predictions presented here can be accessed by typing the species name in the collection.

Specific calculat–ons:

```
% LWw - wet weight calculation from Fonds water content formula

Wd = (LWw(:,1)*del_M).^3 * (1 + f_Deniel * w)* d_V; % g, expected dry weight at time
```

Kd = 100*Wd./LWw(:,1).^3; % -, Fulton's dry index condition

dry_content = 40.68 * Kd .^0.364 ./100; % -, dry content

(from Fonds et al. 1989)

EWw = Wd ./dry_content; % g, wet weight at f

Table A3. Model primary parameters for the common sole (*Solea solea*) that were used for the simulations in the main text. Table lists primary and dataset-specific parameters estimated by DEBtool routines (Add-my-Pet procedure), with the exception of Maximum surface area specific assimilation rate, {p_{Am}}, which is a primary parameter calculated as $\{\dot{p}_{Am}\} = \frac{z}{\kappa}\frac{[\dot{p}_M]}{} L_m^{ref}$, where $L_m^{ref} = 1$ cm. Several parameters (v, {p_{Am}}) in the abj-model applied here increase their value between birth and metamorphosis (see Appendix A), so the final value is provided in brackets. The final parameter value is calculated by multiplying the initial value by $s_M = 2.7942$, calculated at $f = 1$. Primary parameters for which default values were used are listed in the table footnote.

Parameter	Symbol	Value	Unit
Arrhenius temperature	T_A	7980	K
Zoom factor (female) *	z	7.069	-
* Maximum surface area specific assimilation rate (female)	{p_{Am}}	282.195 (788.5219)	J/d·cm$^{2;}$
Zoom factor (male) **	z_m	6.53	-
** Maximum surface area specific assimilation rate (male)	{p_{Am}}$_m$	260.6845 (728.4164)	J/d·cm$^{2;}$
Energy conductance	v	0.06828 (0.1908)	cm/d
Allocation fraction to soma (kappa)	κ	0.782	-
Volume specific somatic maintenance	[p_M]	31.22	J/d·cm^3
Specific cost for structure	[E_G]	5188	J/cm^3
Maturity at hatching	E_H^h	0.1809	J
Maturity at birth	E_H^b	0.3417	J
Maturity at end of metamorphosis	E_H^j	7.49	J
Maturity at puberty	E_H^p	1.964×10^5	J
Weibull aging acceleration (female)	h_a	3.843×10^{-9}	d^{-2}
Weibull aging acceleration (male)	h_{am}	4.5122×10^{-9}	d^{-2}
Arrhenius temperature for high temperature extreme	T_{AH}	20,300	K
High temperature extreme	T_H	293.2	K (20.05 °C)
Shape coefficient for larvae	δ_{Me}	0.1578	-
Shape coefficient post-metamorphosis	δ_M	0.199	-

Standard parameter values from Kooijman (2010) [20]: Maximum specific searching rate, {F_m} = 6.5 d^{-1}·cm^{-2}; Digestion efficiency of food to reserve, $\cdot\kappa_X = 0.8$; Digestion efficiency of food to faeces, $\kappa_P = 0.1$; Reproduction efficiency, $\kappa_R = 0.95$; Maturity maintenance rate coefficient $k_J = 0.002$ d^{-1}; Gompertz stress coefficient, $s_G = 0.0001$; Specific density of structure and reserve, $d_V = d_E = 0.2$ g/cm^3.

Table A4. Life-history traits ('zero-variate data') of common sole (*S. solea*) used for model parameterization, with corresponding sources, model predictions, and relative errors. Life-history traits are grouped into life stages; '*Birth*' is defined in DEB as 'onset of feeding', and thus corresponds with mouth opening of sole larvae. *Definitions of age*: '*Age at hatching*' corresponds to incubation duration (from fertilization until hatching); '*Age at birth*' corresponds to days needed from fertilization until mouth opening, and '*Age at metamorphosis*' corresponds to time elapsed between birth (mouth opening) and end of metamorphosis. When relevant, temperatures are listed in the last column under Notes. Unless otherwise specified, the scaled functional response f for certain life-history traits matches that for corresponding datasets: e.g., f for larval age and length data in this Table and sourced from [41] is the same as f for larval growth curves from [41] in Figure S2.1. References for sources (in square brackets) are listed in the general Reference list.

Life-History Trait (Unit)	Data	Prediction	Relative Error (%)	Note, Source
Hatching				
Age (d)	4.25	4.842	7.59	Incubation at 13 °C; [41]
Length (cm)	0.325	0.316	2.63	[41]
Weight, dry (µg)	51.9	35.69	31.23	Figure 1, age-weight relationship [40]
Birth (mouth opening)				
Age (d)	8	7.506	6.17	Incubation and rearing at 13 °C [41]
Length (cm)	0.425	0.391	8.02	[41]
Weight, dry (µg)	91.96	67.28	26.84	Figure 1, [40]
Metamorphosis (end)				
Age (d)	28	25.43	9.19	Rearing at 13 °C [41]
Length (cm)	1	0.865	13.52	[41]
Weight, dry (mg)	1.8	1.934	7.45	control at 12 °C Figure 1A, in [93], f assumed as in [41]
Puberty				
Age, female (yr)	2.58	2.18	15.37	Average temp 13 °C, number based on smallest spawning females maturing a year earlier [94]
Age, female (yr)	3	2.93	2.20	Average temp 13 °C, 50% of age 3 are mature, temp is North Sea estimate [95]
Age, male (yr)	1.94	1.95	0.62	Average temp assumed 13 °C; age calculated from length [96] via age-length relationship [94]
Length, female (cm)	27	23.03	14.69	Number based on smallest spawning females maturing a year earlier [94]
Length, male (cm)	22	19.86	9.81	[96]
Weight, wet, female (g)	173	117.6	32.02	length-gonad-free weight relationship for female estimated from raw dataset from [94]: Wwp_soma = 0.0041 × L_p^3.2312', in accordance with 200 g from [95] (f ~0.6, T = 10 (North sea guestimates)
Weight, wet, male (g)	87	74.21	14.7	length-gonad-free weight relationship for male estimated from raw dataset from [94]: Wwpm_soma = 0.004 × L_{pm}^3.2304'
Ultimate				
Lifespan, female (yr)	26	25.93	0.24	Average temp assumed 13 °C, Table 118, [94] p.383
Lifespan, male (yr)	24	23.94	0.26	Average temp assumed 13 °C, Table 119, [94] p.384
Length, female (cm)	48	49.92	4.0	estimate [94] p.387; North Sea specimen rarely above 45 cm [97], but reports of 70 cm specimen exist
Length, male (cm)	42	46.12	9.81	estimate [94] p.387

Table A4. *Cont.*

Life-History Trait (Unit)	Data	Prediction	Relative Error (%)	Note, Source
Weight, wet, female (g)	1110	1197	7.89	length-gonad-free weight relationship for female estimated from raw dataset from [94] Wwi_soma = 0.0041 × Li^3.2312, Ultimate wet weight in fishbase is 3000 g
Weight, wet, male (g)	701	929.5	32.6	length-gonad-free weight relationship for male estimated from raw dataset from [94]: Wwi_soma = 0.004 × Li_m^3.2304
Reproduction				
Fecundity (eggs/day)	3014	1601	46.88	At length = 45 cm, average temp 10 °C, [98]
Fecundity (eggs/day)	3027	1927	36.33	At max length, p.243 length-fecundity relationship, assumed average temp 13 °C [94]
Energy in an egg (J)	2	2.06	3.05	mean of batches with 100% viability from wild fish: 13.3% of dry weight is total lipids (assume 37,500 J·g d^{-1}) and 65.9% is crude proteins (assume 18,000 J·g d^{-1}) => E0 = Wd0 × (0.133 × 37500 + 0.659 × 18000); [66]
Egg weight, dry (µg)	1.2	0.89	25.37	Wd0; Figure 5 (Page 137) for an egg diameter of 1.4 mm, 1000 eggs = 0.12 g, experimental data with in situ genitors [66]
Ingestion (pseudodata)				
Max surf.area specific assimilation rate, $\{pAm\}_I$ (J/d·cm^2)	800	788.7	1.41	Approximated from mean daily food consumption of dry mussel meat as function of total wet weight, length-weight relationship, and energy density of mussel meat; assumed at T_{ref} = 20 °C [99]

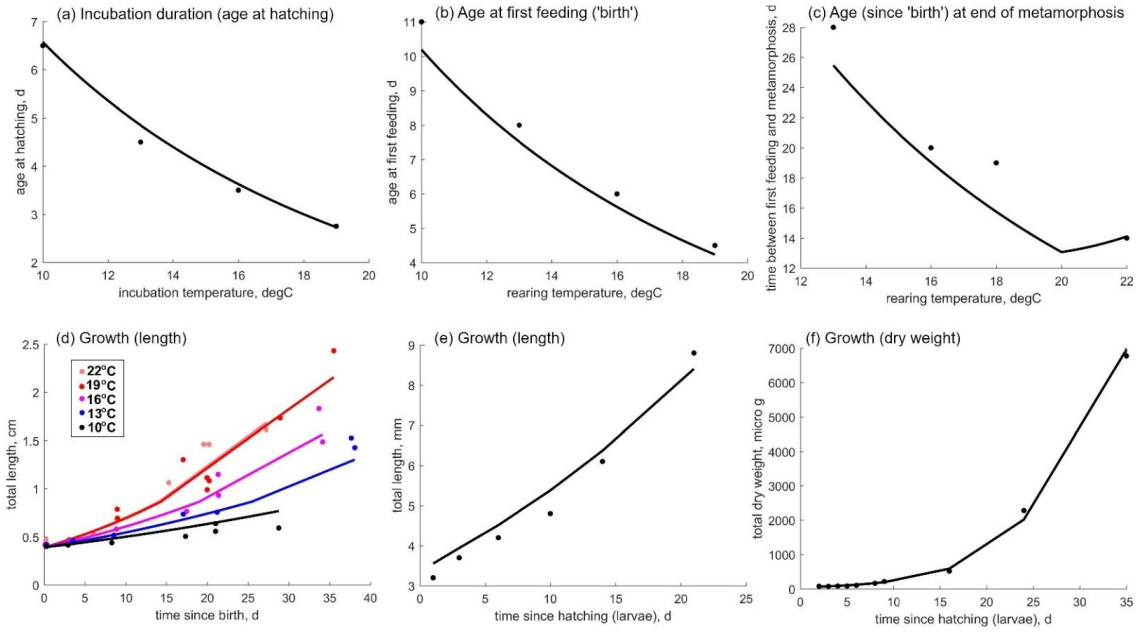


Figure A1. Larval development and growth of *S. solea*. (**a**–**c**): duration of developmental stages as a function of incubation or rearing temperature; (**d**–**f**): larval growth in total length and dry weight over time. *Data sources and corresponding conditions* (estimated scaled functional response *f*, simulated temperature T): Panels a-d: [41] (*f* = 0.4451, T = 10, 13, 16, 19 °C for panels (**a**,**b**), T = 13, 16, 18, and 22 °C for panel (**c**), and T = 10, 13, 16, 19, 22 °C for panel (**d**)); Panel (**e**): [100] (*f* = 0.305, T = 11.2 °C for incubation (fertilization to hatching), 16.1 °C from hatching to birth, and 19.1 °C from birth onward; Panel (**f**): [40]—mean values (*f* = 0.4813, T = 12 °C for incubation (fertilization to hatching), then T = 15 °C).

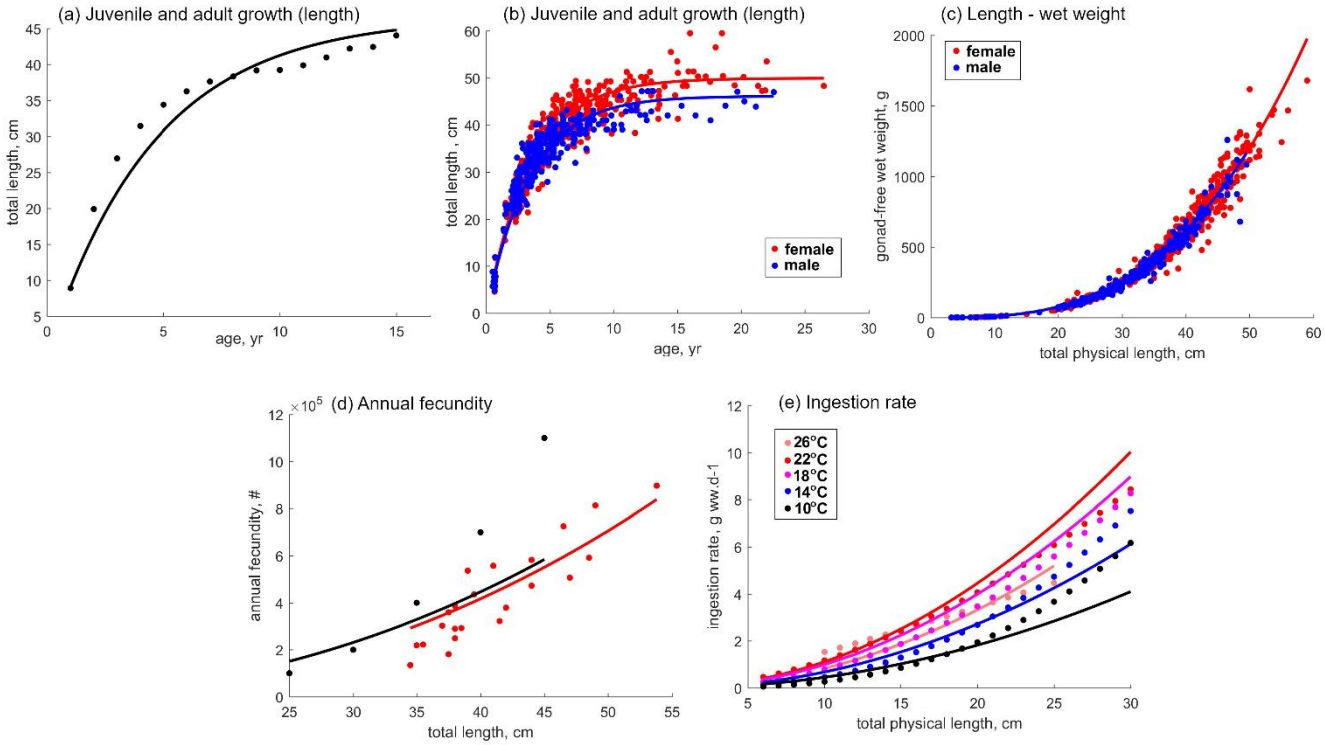


Figure A2. Juvenile and adult *S. solea*. (**a**): growth in total length, sex unspecified; (**b**): growth in total length, females and males separated; (**c**): Relationship of length and gonad free wet weight, for males and females. (**d**): Relationship of length and annual egg production. (**e**): Ingestion rate as a function of length and temperature. *Dara sources and corresponding conditions* (estimated scaled functional response f, simulated temperature T): Panel (**a**): [100] (f = 0.4703, T = 10 °C); Panels (**b**,**c**) and red dots in panel (**d**): [94] (f = 0.5037, T = 13 °C); Panel (**d**) (black dots): [98] (f = 1.664, T = 10 °C), Panel (**e**): [Fond1977] (f = 1.156, T = 10, 14, 18, 22, 26 °C; food = mussel meat, energy density of mussels = 18750 J·g dry^{-1} (Fond1989), water content of mussels estimated 80%).

Appendix B.2. Solea Senegalensis AmP Entry

Model parameters are listed in Table A5. The model for *S. senegalensis* was parameterized using data listed in Table A6 and Figures A3 and A4. COMPLETE = 3.3; MRE = 0.117; SMAE = 0.126; SMSE = 0.046. The parameter set, data, and predictions presented here can be accessed by typing the species name in the collection.

Table A5. Model primary parameters for the senegalese sole (*Solea senegalensis*) that were used for the simulations in the main text. The table lists primary and dataset specific parameters estimated by DEBtool routines (Add-my-Pet procedure), with the exception of Maximum surface area specific assimilation rate, $\{p_{Am}\}$, that is a primary parameter calculated as $\{\dot{p}_{Am}\} = \frac{z}{\kappa}\frac{[\dot{p}_M]}{} L_m^{ref}$, where $L_m^{ref} = 1$ cm. Several parameters (v, $\{p_{Am}\}$) in the abj-model applied here increase their value between birth and metamorphosis (see Appendix A), so the final value is provided in brackets. The final parameter value is calculated by multiplying the initial value by s_M = 3.3472 calculated at f = 1. Primary parameters for which default values were used are listed in the table footnote.

Parameter	Symbol	Value	Unit
Arrhenius temperature	T_A	6528	K
Zoom factor (female) *	z	3.399	-
* Maximum surface area specific assimilation rate (female)	$\{p_{Am}\}$	95.61 (320.05)	J/d·cm^2

Table A5. *Cont.*

Parameter	Symbol	Value	Unit
Zoom factor (male) **	z_m	3.071	-
** Maximum surface area specific assimilation rate (male)	$\{p_{Am}\}$	86.37 (289.11)	J/d·cm^2
Energy conductance	v	0.0697 (0.2332)	cm/d
Allocation franction to soma (kappa)	κ	0.8117	-
Volume specific somatic maintenance	$[p_M]$	22.83	J/d·cm^3
Specific cost for structure	$[E_G]$	5230	J/cm^3
Maturity at hatching	E_H^h	0.0552	J
Maturity at birth	E_H^b	0.1671	J
Maturity at end of metamorphosis	E_H^j	6.309	J
Maturity at puberty	E_H^p	1.258×10^6	J
Weibull aging acceleration (female)	h_a	5.776×10^{-9}	d^{-2}
Weibull aging acceleration (male)	h_{am}	4.5122×10^{-9}	d^{-2}
Shape coefficient for larvae	δ_{Me}	0.221	-
Shape coefficient post-metamorphosis	δ_M	0.2235	-

Standard parameter values from Kooijman (2010) [20]: Maximum specific searching rate, $\{F_m\}$ = 6.5 d^{-1}·cm^{-2}; Digestion efficiency of food to reserve, $\cdot\kappa_X$ = 0.8; Digestion efficiency of food to feces, κ_P = 0.1; Reproduction efficiency, κ_R = 0.95; Maturity maintenance rate coefficient k_J = 0.002 d^{-1}; Gompertz stress coefficient, s_G = 0.0001; Specific density of structure and reserve, $d_V = d_E$ = 0.2 g/cm^3.

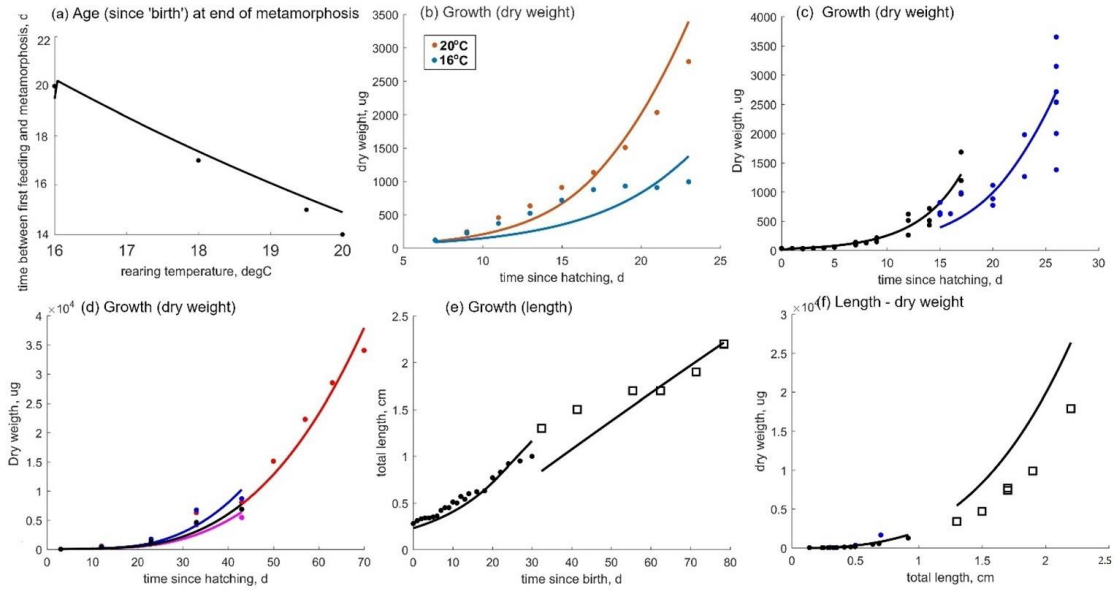


Figure A3. Larval development and growth of *S. senegalensis*. (**a**): duration of development (from mouth opening to completion of metamorphosis) as a function of rearing temperature; (**b**–**e**): larval and juvenile growth in total length and dry weight over time; (**f**): length-dry weight relationship for larvae and metamorphosized juveniles. *Data sources and corresponding conditions* (estimated scaled functional response *f*, simulated temperature T): Panel (**a**): [102] (f = 1, T = 20 °C (constant) and 16 °C (non-constant: 0–6 dph 20 °C, 6 dph 18 °C, 7 dph onwards 16 °C), [103](f = 0.820, T = 18 °C), [58] (f = 1, T = 19.5 °C); Panel (**b**): [102] (f = 1, T = 20 °C constant or gradually reduced to T = 16 °C); Panel (**c**): [58] black dots (f = 1.05, T = 19.5 °C) and [104] blue dots (f = 0.799, T = 19.5 °C); Panel (**d**): [105] different food quality and quantity (f = 0.651—red; f = 0.61—pink, f = 0.71—blue, f = 0.651—black, T = 19.5 °C); Panel (**e**): [103] dots (f = 0.82, T = 18 °C), [106] squares (f = 0.47, T = 20 °C); Panel (**f**): [107] blue dots (f = 1) [58] black dots (f = 1), [106] squares (f = 0.47).

Table A6. Life-history traits ('zero-variate data') of Senegalese sole (*S. senegalensis*) used for model parameterization, with corresponding sources, model predictions, and relative errors. Life-history traits are grouped into life stages; '*Birth*' is defined in DEB as 'onset of feeding', and thus corresponds with mouth opening of sole larvae. *Definitions of age*: '*Age at hatching*' corresponds to incubation duration (from fertilization until hatching); '*Age at birth*' corresponds to days needed from fertilization until mouth opening, and '*Age at metamorphosis*' corresponds to time elapsed between birth (mouth opening) and end of metamorphosis. When relevant, temperatures are listed in the last column under Notes. Unless otherwise specified, the scaled functional response f for certain life-history traits matches that for corresponding datasets. References for sources (in square brackets) are listed in the general Reference list.

Life-History Trait (Unit)	Data	Prediction	Relative Error (%)	Note, Source
Hatching				
Age (d)	1.583	1.724	8.83	38 h, Incubation at 19.5 °C [58]
Length (cm)	0.224	0.1595	28.8	[58]
Weight, dry (µg)	33.19	41.89	26.21	[58]
Birth (mouth opening)				
Age (d)	3.6	3.43	4.71	mouth opening 2 days after hatching, rearing at 19.5 °C [58]
Length (cm)	0.2484	0.2308	7.1	[58]
Weight, dry (µg)	30	35.65	18.83	[58]
Metamorphosis (end)				
Age (d)	19	18.89	0.57	Start 16 dpf (14 dph), end 19 dpf (17 dph), rearing at 19.5 °C [58]
Length (cm)	0.9176	0.7816	14.82	At start of metamorphosis L = 0.6857 cm [58]
Weight, dry (mg)	1.28	1.35	5.58	At start of metamorphosis Wd = 0.553 mg [58]
Puberty				
Age (yr)	1460	1439	1.45	Average temp 17.5 °C (between 15 °C and 20 °C in Tagus estuary) [101]
Length, female (cm)	38	39.02	2.69	[102]
Length, male (cm)	33	35.29	6.92	[102]
Weight, wet, female (g)	850	832.3	2.08	[102]
Weight, wet, male (g)	650	601.6	7.44	[102]
Ultimate				
Lifespan (yr)	4015	4000	0.38	Average temp 17.5 °C [62]
Length (cm)	52	51.5	0.97	Average size around 40 cm, max ever recorded 70 cm, FAO [62]
Weight, wet (g)	1830	1913	4.51	Average weight of male and female [102]
Reproduction				
Fecundity (eggs/day)	4160	4155	0.11	At ultimate length and average temp 18.5 °C, calculated as total weight of eggs daily collected during the spawning seasons of 1996 and 1997 divided by Wd of egg and 365 [30]
Energy in an egg (J)	1	1.078	7.8	[58]
Egg weight, dry (µg)	46.1	46.8	1.5	[58]
Egg diameter (cm)	0.1	0.071	23.52	[58]

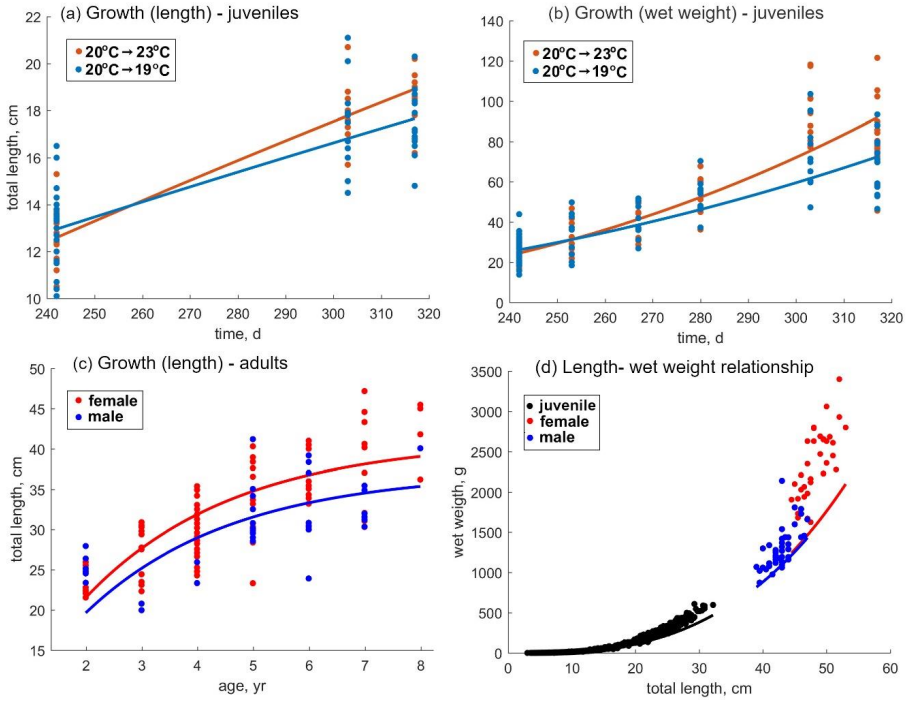


Figure A4. Juvenile and adult growth of *S. senegalensis*. (**a**,**b**) juvenile growth in total length and wet weight over time; (**c**): adult (male, female) growth in total length over time; (**d**): length-wet weight relationship for juveniles and adults (male, female). *Data sources and corresponding conditions* (estimated scaled functional response *f*, simulated temperature T): Panels (**a**,**b**): [108] (f = 1.49, T = 20 °C from birth until start of experiment, 19 °C or 23 °C thereafter); Panel (**c**): [62] (f = 0.80, T = 17.5 °C); Panel (**d**): [102] (f = 1).

Appendix C. Additional Results

			Solea senegalensis					*Solea solea*				
	Spawn	Stage	Age (dpf)	Size (cm)	Stage duration (days)	Growth rate (cm/d)	Variation from baseline (days)	Age (dpf)	Size (cm)	Stage duration (days)	Growth rate (cm/d)	Variation from baseline (days)
S1 - Baseline	Early	ah	3.5	0.18	3.5			6.6	0.35	6.6		
		ab	7.1	0.27	3.5			10.3	0.45	3.7		
		aj	38.2	0.79	31.1	0.086		37.0	0.87	26.7	0.041	
		ap	2258.8	38.01	2220.6	0.021		499.4	23.67	462.4	0.053	
	Mid	ah	2.2	0.18	2.2			7.8	0.35	7.8		
		ab	4.4	0.27	2.2			12.0	0.45	4.3		
		aj	28.0	0.79	23.6	0.117		37.8	0.87	25.7	0.040	
		ap	2257.6	37.99	2229.6	0.021		464.2	23.67	426.4	0.057	
	Late	ah	1.7	0.18	1.7			5.1	0.35	5.1		
		ab	3.4	0.27	1.7			7.8	0.45	2.8		
		aj	24.9	0.79	21.5	0.132		23.5	0.87	15.7	0.064	
		ap	2254.7	37.99	2229.8	0.021		436.5	23.67	413	0.060	
S2 - 50% decrease	Early	ah	3.6	0.18	3.6		0	6.6	0.35	6.6		0
		ab	7.3	0.27	3.7		0.2	10.5	0.45	3.9		0.2
		aj	40.8	0.79	33.6	0.080	2.6	40.1	0.87	29.6	0.038	3.2
		ap	3427.9	36.56	3387.1	0.013	1169.1	540.8	23.44	500.6	0.048	41.4
	Mid	ah	2.2	0.18	2.2		0	7.8	0.35	7.8		0
		ab	4.5	0.27	2.3		0.1	12.3	0.45	4.5		0.2
		aj	30.9	0.78	26.4	0.106	2.9	40.3	0.87	28	0.037	2.5
		ap	3442.0	36.54	3411.1	0.013	1184.4	504.1	23.44	463.8	0.052	39.9
	Late	ah	1.7	0.18	1.7		0	5.1	0.35	5.1		0
		ab	3.5	0.27	1.8		0.1	8.0	0.45	2.9		0.2
		aj	27.8	0.78	24.3	0.118	2.9	25.2	0.86	17.2	0.060	1.6
		ap	3548.2	36.53	3520.4	0.013	1293.5	480.2	23.44	455	0.054	43.7
S3 - 50% increase	Early	ah	3.5	0.18	3.5		0	6.6	0.35	6.6		0
		ab	7.0	0.27	3.5		-0.1	10.2	0.45	3.6		-0.1
		aj	37.3	0.79	30.3	0.088	-0.9	35.8	0.87	25.6	0.042	-1.1
		ap	1980.3	38.44	1943	0.024	-278.6	481.0	23.74	445.1	0.055	-18.4
	Mid	ah	2.2	0.18	2.2		0	7.7	0.35	7.7		0
		ab	4.4	0.27	2.2		0	11.9	0.45	4.2		-0.1
		aj	27.0	0.79	22.6	0.122	-1	36.8	0.87	24.9	0.041	-0.9
		ap	1977.6	38.44	1950.6	0.024	-280	451.0	23.75	414.2	0.059	-13.2
	Late	ah	1.7	0.18	1.7		0	5.1	0.35	5.1		0
		ab	3.4	0.27	1.7		0	7.8	0.45	2.7		-0.1
		aj	24.0	0.79	20.5	0.137	-1	23.0	0.87	15.2	0.066	-0.6
		ap	2069.8	38.43	2045.8	0.023	-184.9	423.4	23.74	400.4	0.062	-13.1

Food availability

Figure A5. *Cont*.

				Solea senegalensis					*Solea solea*				
Temperature	S1 - Baseline		ab	7.1	0.27	3.5			10.3	0.45	3.7		
			aj	38.2	0.79	31.1	0.086		37.0	0.87	26.7	0.041	
			ap	2261.4	38.00	2223.2	0.021		499.4	23.67	462.4	0.053	
		Mid	ah	2.2	0.18	2.2			7.8	0.35	7.8		
			ab	4.4	0.27	2.2			12.0	0.45	4.3		
			aj	28.0	0.79	23.6	0.117		37.8	0.87	25.7	0.040	
			ap	2258.2	37.98	2230.2	0.021		464.2	23.67	426.4	0.057	
		Late	ah	1.7	0.18	1.7			5.1	0.35	5.1		
			ab	3.4	0.27	1.7			7.8	0.45	2.8		
			aj	24.9	0.79	21.5	0.132		23.5	0.87	15.7	0.064	
			ap	2249.6	38.00	2224.7	0.021		436.3	23.67	412.8	0.060	
	S4 - RCP 4.5	Early	ah	2.8	0.18	2.8		-0.8	5.3	0.35	5.3		-1.3
			ab	5.6	0.27	2.8		-1.5	8.3	0.45	3		-2
			aj	33.3	0.79	27.7	0.099	-4.9	29.2	0.87	21	0.052	-7.7
			ap	1979.5	38.00	1946.2	0.024	-281.9	465.7	23.67	436.5	0.057	-33.6
		Mid	ah	1.8	0.18	1.8		-0.4	6.2	0.35	6.2		-1.6
			ab	3.6	0.27	1.8		-0.8	9.6	0.45	3.4		-2.5
			aj	25.3	0.79	21.7	0.130	-2.7	30.7	0.87	21.2	0.049	-7
			ap	1989.5	37.97	1964.2	0.024	-268.7	441.7	23.67	411	0.060	-22.5
		Late	ah	1.6	0.18	1.6		-0.1	4.1	0.35	4.1		-0.9
			ab	3.2	0.27	1.6		-0.3	6.4	0.45	2.3		-1.4
			aj	23.8	0.79	20.6	0.138	-1.1	19.8	0.87	13.4	0.076	-3.8
			ap	2020.5	38.00	1996.6	0.023	-229.1	420.6	23.67	400.9	0.063	-15.7
	S5 - RCP 8.5	Early	ah	2.2	0.18	2.2		-1.3	4.3	0.35	4.3		-2.3
			ab	4.4	0.27	2.2		-2.6	6.7	0.45	2.4		-3.6
			aj	28.7	0.79	24.2	0.114	-9.5	23.3	0.87	16.7	0.065	-13.6
			ap	1849.7	38.00	1821	0.026	-411.7	440.8	23.67	417.4	0.060	-58.6
		Mid	ah	1.6	0.18	1.6		-0.6	4.9	0.35	4.9		-2.8
			ab	3.2	0.27	1.6		-1.2	7.6	0.45	2.7		-1.9
			aj	24.0	0.79	20.7	0.137	-4	25.0	0.87	17.3	0.060	-12.8
			ap	1853.5	37.98	1829.5	0.026	-404.7	426.2	23.67	401.2	0.062	-38
		Late	ah	1.5	0.18	1.5		-0.2	3.4	0.35	3.4		-1.7
			ab	3.1	0.27	1.6		-0.4	5.3	0.45	1.9		-2.6
			aj	23.5	0.79	20.5	0.140	-1.4	16.5	0.87	11.3	0.091	-7
			ap	1846.8	38.00	1823.3	0.026	-402.8	413.1	23.67	396.5	0.064	-23.3
Food x Temperature	S1 - Baseline	Early	ah	3.6	0.18	3.6			6.6	0.35	6.6		
			ab	7.3	0.27	3.7			10.5	0.45	3.9		
			aj	40.8	0.79	33.6	0.080		40.1	0.87	29.6	0.038	
			ap	3427.9	36.56	3387.1	0.013		540.8	23.44	500.6	0.048	
		Mid	ah	2.2	0.18	2.2			7.8	0.35	7.8		
			ab	4.5	0.27	2.3			12.3	0.45	4.5		
			aj	30.9	0.78	26.4	0.106		40.3	0.87	28	0.037	
			ap	3442.0	36.54	3411.1	0.013		504.1	23.44	463.8	0.052	
		Late	ah	1.7	0.18	1.7			5.1	0.35	5.1		
			ab	3.5	0.27	1.8			8.0	0.45	2.9		
			aj	27.8	0.78	24.3	0.118		25.2	0.86	17.2	0.060	
			ap	3548.2	36.53	3520.4	0.013		480.2	23.44	455	0.054	
	S6 - 50% decrease_RCP 4.5	Early	ah	2.8	0.18	2.8		-0.8	5.3	0.35	5.3		-1.3
			ab	5.7	0.27	2.9		-1.6	8.4	0.45	3.1		-2.1
			aj	35.9	0.78	30.2	0.091	-5	31.9	0.86	23.5	0.047	-8.2
			ap	3067.6	36.55	3031.8	0.015	-360.3	513.4	23.44	481.5	0.051	-27.4
		Mid	ah	1.8	0.18	1.8		-0.4	6.2	0.35	6.2		-1.6
			ab	3.7	0.27	1.9		-0.8	9.8	0.45	3.6		-2.5
			aj	28.2	0.78	24.4	0.116	-2.7	33.0	0.86	23.3	0.046	-7.3
			ap	3139.7	36.50	3111.5	0.014	-302.3	481.8	23.44	448.8	0.054	-22.3
		Late	ah	1.6	0.18	1.6		-0.1	4.2	0.35	4.2		-0.9
			ab	3.3	0.27	1.7		-0.3	6.5	0.45	2.4		-1.4
			aj	26.7	0.78	23.4	0.123	-1.1	21.2	0.86	14.7	0.071	-4
			ap	3142.7	36.53	3116	0.014	-405.5	469.4	23.44	448.2	0.056	-10.8
	S7 - 50% decrease_RCP 8.5	Early	ah	2.2	0.18	2.2		-1.3	4.3	0.35	4.3		-2.3
			ab	4.5	0.27	2.3		-2.7	6.8	0.45	2.5		-3.7
			aj	31.6	0.78	27.1	0.104	-9.2	25.4	0.86	18.6	0.059	-14.7
			ap	2799.1	36.55	2767.4	0.016	-628.9	490.9	23.44	465.5	0.053	-49.9
		Mid	ah	1.6	0.18	1.6		-0.6	4.9	0.35	4.9		-2.8
			ab	3.3	0.27	1.7		-1.2	7.8	0.45	2.9		-4.5
			aj	26.8	0.78	23.5	0.122	-4.1	26.9	0.86	19.1	0.056	-13.4
			ap	2850.7	36.54	2823.8	0.016	-591.4	465.9	23.44	439	0.056	-38.2
		Late	ah	1.5	0.18	1.5		-0.2	3.4	0.35	3.4		-1.7
			ab	3.1	0.27	1.6		-0.4	5.4	0.45	2		-2.6
			aj	26.4	0.78	23.3	0.124	-1.4	17.8	0.86	12.4	0.085	-7.4
			ap	2853.6	36.55	2827.2	0.016	-694.6	470.0	23.44	452.2	0.056	-10.2

Figure A5. Predicted age and size at different stages, stage duration and growth rates for *Solea* spp. for the evaluated effects of temperature and food availability. In total, we simulated seven scenarios (S1–S7), with three spawning events (early-mid-late) in each. Scenarios were designed to reflect potential changes in food availability and increase in temperature (warming of 1.8 and 3.7 degrees—RCP 4.5 and RCP 8.5, respectively, IPCC, 2014), both relative to the baseline, i.e., current conditions. Current (baseline) food availability (X) is assumed to result in scaled functional response f = 0.85 in both species, and temperature is assumed to reflect the average seasonal fluctuations in typical coastal sea and estuaries inhabited by soles (please see Methods of main text for more information).

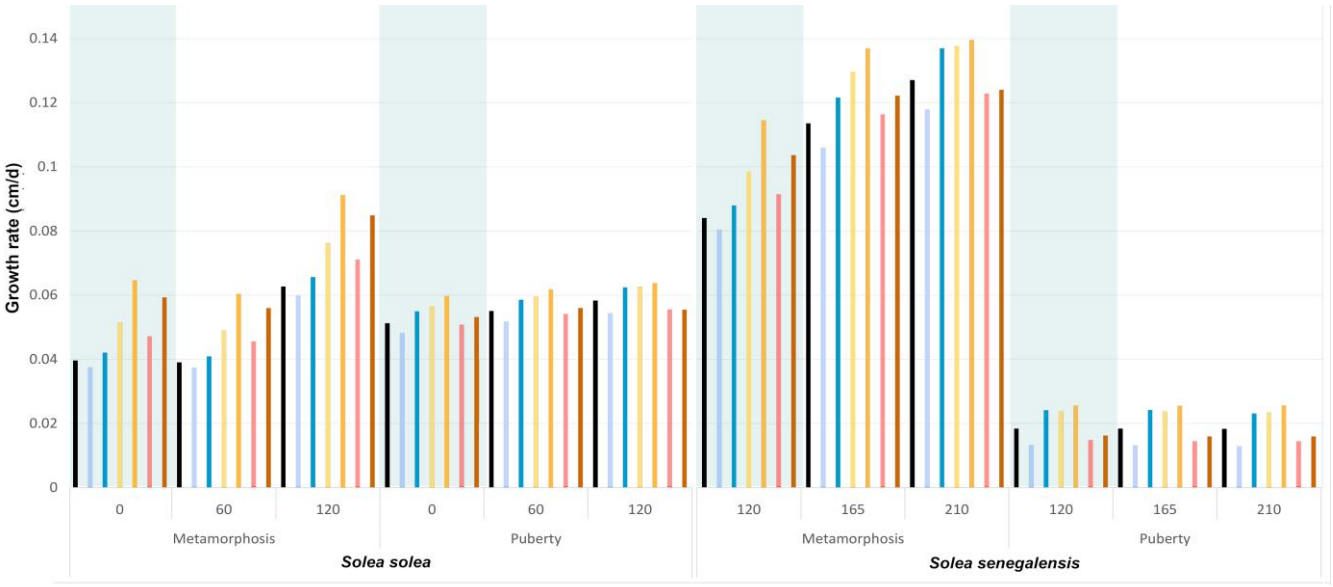


Figure A6. Growth rates in *Solea* spp. larvae (from hatching until complete metamorphosis) and juveniles (from metamorphosis until maturation). Green rectangles mark the individuals that spawned the earliest, with date of spawning indicated as the day of the year (number) under the bars. Colors of the bars correspond to color-coding of scenarios (S) in Figures 5 and 6 of the manuscript: black—S1 baseline, blue—S2 and S3 food availability modifications, yellow—S4 and S5 temperature increase, red—S6 and S7 food decrease combined with temperature increase. For scenario descriptions please see Table 1 of the manuscript.

References

1. Hermant, M.; Lobry, J.; Bonhommeau, S.; Poulard, J.-C.; Le Pape, O. Impact of warming on abundance and occurrence of flatfish populations in the Bay of Biscay (France). *J. Sea Res.* **2010**, *64*, 45–53. [CrossRef]
2. Petrik, C.M.; Stock, C.A.; Andersen, K.H.; van Denderen, P.D.; Watson, J.R. Large Pelagic Fish Are Most Sensitive to Climate Change Despite Pelagification of Ocean Food Webs. *Front. Mar. Sci.* **2020**, *7*, 588482. [CrossRef]
3. Cabral, H.; Drouineau, H.; Teles-Machado, A.; Pierre, M.; Lepage, M.; Lobry, J.; Reis-Santos, P.; Tanner, S.E. Contrasting impacts of climate change on connectivity and larval recruitment to estuarine nursery areas. *Prog. Oceanogr.* **2021**, *196*, 102608. [CrossRef]
4. Bueno-Pardo, J.; Nobre, D.; Monteiro, J.N.; Sousa, P.M.; Costa, E.F.S.; Baptista, V.; Ovelheiro, A.; Vieira, V.M.N.C.S.; Chícharo, L.; Gaspar, M.; et al. Climate change vulnerability assessment of the main marine commercial fish and invertebrates of Portugal. *Sci. Rep.* **2021**, *11*, 2958. [CrossRef] [PubMed]
5. Bolle, L.; Dickey-Collas, M.; van Beek, J.; Erftemeijer, P.; Witte, J.; van der Veer, H.; Rijnsdorp, A. Variability in transport of fish eggs and larvae. III. Effects of hydrodynamics and larval behaviour on recruitment in plaice. *Mar. Ecol. Prog. Ser.* **2009**, *390*, 195–211. [CrossRef]
6. Richon, C.; Aumont, O.; Tagliabue, A. Prey Stoichiometry Drives Iron Recycling by Zooplankton in the Global Ocean. *Front. Mar. Sci.* **2020**, *7*, 451. [CrossRef]
7. Richardson, A.J. In hot water: Zooplankton and climate change. *ICES J. Mar. Sci.* **2008**, *65*, 279–295. [CrossRef]
8. Sydeman, W.J.; Poloczanska, E.; Reed, T.E.; Thompson, S.A. Climate change and marine vertebrates. *Science* **2015**, *350*, 772–777. [CrossRef] [PubMed]
9. Van de Waal, D.B.; Litchman, E. Multiple global change stressor effects on phytoplankton nutrient acquisition in a future ocean. *Philos. Trans. R. Soc. B Biol. Sci.* **2020**, *375*, 20190706. [CrossRef] [PubMed]
10. Edwards, M.; Richardson, A.J. Impact of climate change on marine pelagic phenology and trophic mismatch. *Nature* **2004**, *430*, 881–884. [CrossRef]
11. Poloczanska, E.S.; Brown, C.J.; Sydeman, W.J.; Kiessling, W.; Schoeman, D.S.; Moore, P.J.; Brander, K.; Bruno, J.F.; Buckley, L.B.; Burrows, M.T.; et al. Global imprint of climate change on marine life. *Nat. Clim. Change* **2013**, *3*, 919–925. [CrossRef]
12. Vagner, M.; Zambonino-Infante, J.-L.; Mazurais, D. Fish facing global change: Are early stages the lifeline? *Mar. Environ. Res.* **2019**, *147*, 159–178. [CrossRef] [PubMed]
13. Fincham, J.I.; Rijnsdorp, A.D.; Engelhard, G.H. Shifts in the timing of spawning in sole linked to warming sea temperatures. *J. Sea Res.* **2013**, *75*, 69–76. [CrossRef]
14. Rijnsdorp, A.D.; Peck, M.A.; Engelhard, G.H.; Möllmann, C.; Pinnegar, J.K. Resolving the effect of climate change on fish populations. *ICES J. Mar. Sci.* **2009**, *66*, 1570–1583. [CrossRef]

15. Belanger, S.E.; Balon, E.K.; Rawlings, J.M. Saltatory ontogeny of fishes and sensitive early life stages for ecotoxicology tests. *Aquat. Toxicol.* **2010**, *97*, 88–95. [CrossRef] [PubMed]
16. Hutchinson, T.H.; Solbe, J.; Kloepper-Sams, P.J. Analysis of the ECETOC aquatic toxicity (EAT) database III—Comparative toxicity of chemical substances to different life stages of aquatic organisms. *Chemosphere* **1998**, *36*, 129–142. [CrossRef]
17. Houde, E.D. Emerging from Hjort's Shadow. *J. Northwest Atl. Fish. Sci.* **2008**, *41*, 53–70. [CrossRef]
18. Jusup, M.; Sousa, T.; Domingos, T.; Labinac, V.; Marn, N.; Wang, Z.; Klanjšček, T. Physics of metabolic organization. *Phys. Life Rev.* **2017**, *20*, 1–39. [CrossRef]
19. Kearney, M.R. What is the status of metabolic theory one century after Pütter invented the von Bertalanffy growth curve? *Biol. Rev.* **2021**, *96*, 557–575. [CrossRef] [PubMed]
20. Kooijman, S.A.L.M. *Dynamic Energy Budget Theory for Metabolic Organisation*, 3rd ed.; Cambridge University Press: New York, NY, USA, 2010; Volume 365, ISBN 9780521131919.
21. Sousa, T.; Domingos, T.; Kooijman, S.A.L.M. From empirical patterns to theory: A formal metabolic theory of life. *Philos. Trans. R. Soc. B Biol. Sci.* **2008**, *363*, 2453–2464. [CrossRef] [PubMed]
22. Bjørndal, T.; Guillen, J.; Imsland, A. The potential of aquaculture sole production in Europe: Production costs and markets. *Aquac. Econ. Manag.* **2016**, *20*, 109–129. [CrossRef]
23. Cerdà, J.; Manchado, M. Advances in genomics for flatfish aquaculture. *Genes Nutr.* **2013**, *8*, 5–17. [CrossRef]
24. Manchado, M.; Planas, J.V.; Cousin, X.; Rebordinos, L.; Claros, M.G. Current status in other finfish species: Description of current genomic resources for the gilthead seabream (*Sparus aurata*) and soles (*Solea senegalensis* and *Solea solea*). In *Genomics in Aquaculture*; Academic Press: San Diego, CA, USA, 2016; pp. 195–221. ISBN 978-0-12-801418-9. [CrossRef]
25. Anguis, V.; Cañavate, J.P. Spawning of captive Senegal sole (*Solea senegalensis*) under a naturally fluctuating temperature regime. *Aquaculture* **2005**, *243*, 133–145. [CrossRef]
26. Imsland, A.K.; Foss, A.; Conceição, L.E.C.; Dinis, M.T.; Delbare, D.; Schram, E.; Kamstra, A.; Rema, P.; White, P. A review of the culture potential of *Solea solea* and *S. senegalensis*. *Rev. Fish Biol. Fish.* **2003**, *13*, 379–408. [CrossRef]
27. Geffen, A.J.; van der Veer, H.W.; Nash, R.D.M. The cost of metamorphosis in flatfishes. *J. Sea Res.* **2007**, *58*, 35–45. [CrossRef]
28. Sardi, A.E.; Bégout, M.-L.; Cousin, X.; Labadie, P.; Loizeau, V.; Budzinski, H. A review of the effects of contamination and temperature in *Solea solea* larvae. Modeling perspectives in the context of climate change. *J. Sea Res.* **2021**, *176*, 102101. [CrossRef]
29. Campos, C.; Castanheira, M.F.; Engrola, S.; Valente, L.M.P.; Fernandes, J.M.O.; Conceição, L.E.C. Rearing temperature affects Senegalese sole (*Solea senegalensis*) larvae protein metabolic capacity. *Fish Physiol. Biochem.* **2013**, *39*, 1485–1496. [CrossRef] [PubMed]
30. Dinis, M.T.; Ribeiro, L.; Soares, F.; Sarasquete, C. A review on the cultivation potential of *Solea senegalensis* in Spain and in Portugal. *Aquaculture* **1999**, *176*, 27–38. [CrossRef]
31. Cabral, H.; Costa, M.J. Differential Use of Nursery Areas Within the Tagus Estuary by Sympatric Soles, *Solea solea* and *Solea senegalensis*. *Environ. Biol. Fishes* **1999**, *56*, 389–397. [CrossRef]
32. Zambonino-Infante, J.L.; Claireaux, G.; Ernande, B.; Jolivet, A.; Quazuguel, P.; Sévère, A.; Huelvan, C.; Mazurais, D. Hypoxia tolerance of common sole juveniles depends on dietary regime and temperature at the larval stage: Evidence for environmental conditioning. *Proc. R. Soc. B Biol. Sci.* **2013**, *280*, 20123022. [CrossRef]
33. Savina, M.; Lunghi, M.; Archambault, B.; Baulier, L.; Huret, M.; Le Pape, O. Sole larval supply to coastal nurseries: Interannual variability and connectivity at interregional and interpopulation scales. *J. Sea Res.* **2016**, *111*, 1–10. [CrossRef]
34. Schoolfield, R.M.; Sharpe, P.J.H.; Magnuson, C.E. Non-linear regression of biological temperature-dependent rate models based on absolute reaction-rate theory. *J. Theor. Biol.* **1981**, *88*, 719–731. [CrossRef] [PubMed]
35. DEBtool. DEBtool Software Package. 2022. Available online: https://github.com/add-my-pet/DEBtool_M (accessed on 24 November 2022).
36. Kooijman, S.A.L.M.; Pecquerie, L.; Augustine, S.; Jusup, M. Scenarios for acceleration in fish development and the role of metamorphosis. *J. Sea Res.* **2011**, *66*, 419–423. [CrossRef]
37. Marques, G.M.; Augustine, S.; Lika, K.; Pecquerie, L.; Domingos, T.; Kooijman, S.A.L.M. The AmP project: Comparing species on the basis of dynamic energy budget parameters. *PLoS Comput. Biol.* **2018**, *14*, e1006100. [CrossRef]
38. Mounier, F.; Pecquerie, L.; Lobry, J.; Sardi, A.E.; Labadie, P.; Budzinski, H.; Loizeau, V. Dietary bioaccumulation of persistent organic pollutants in the common sole *Solea solea* in the context of global change. Part 1: Revisiting parameterisation and calibration of a DEB model to consider inter-individual variability in experimental and natural conditions. *Ecol. Model.* **2020**, *433*, 109224. [CrossRef]
39. AmPtool. AmPtool Software Package. Available online: https://github.com/add-my-pet/AmPtool (accessed on 24 November 2022).
40. Day, O.J.; Jones, D.A.; Howell, B.R. Food consumption, growth and respiration of sole, *Solea solea* (L.), during early ontogeny in a hatchery environment. *Aquac. Res.* **1996**, *27*, 831–839. [CrossRef]
41. Fonds, M. Laboratory Observations on the Influence of Temperature and Salinity on Development of the Eggs and Growth of the Larvae of *Solea solea*. *Mar. Ecol. Prog. Ser.* **1979**, *1*, 91–99. [CrossRef]
42. Marques, G.M.; Lika, K.; Augustine, S.; Pecquerie, L.; Kooijman, S.A.L.M. Fitting multiple models to multiple data sets. *J. Sea Res.* **2019**, *143*, 48–56. [CrossRef]
43. Sardi, A.E.; Bégout, M.L.; Lalles, A.L.; Cousin, X.; Mounier, F.; Loizeau, V.; Budzinski, H. Temperature and Feeding Frequency Impact the Survival, Growth, and Metamorphosis Success of *Solea solea* Larvae. In revision.

44. Sardi, A.; Omingo, L.; Bégout, M.L.; Cousin, X.; Manchado, M. What Can Go Wrong for Future Senegalensis Sole Recruitment? Studying the Effects of Temperature and Food Availability in Early Life History Traits and Gene Expression of Nutrition and Temperature Stress Genes. In prepress.
45. FAO Solea Solea. Cultured Aquatic Species Information Programme. *FAO Fisheries and Aquaculture Division. Rome*. Text by Colen, R.; Ramalho, A.; Rocha, F.; Dinis, M.T. Available online: https://www.fao.org/fishery/en/culturedspecies/solea_spp/en (accessed on 27 December 2022).
46. Lacroix, G.; Maes, G.E.; Bolle, L.J.; Volckaert, F.A.M. Modelling dispersal dynamics of the early life stages of a marine flatfish (*Solea solea* L.). *J. Sea Res.* **2013**, *84*, 13–25. [CrossRef]
47. Vaz, A.C.; Scarcella, G.; Pardal, M.A.; Martinho, F. Water temperature gradients drive early life-history patterns of the common sole (*Solea solea* L.) in the Northeast Atlantic and Mediterranean. *Aquat. Ecol.* **2019**, *53*, 281–294. [CrossRef]
48. Bachelet, G.; Baron, J.; Blanc, G.; Boschet, C.; Carassou, L.; Chaalali, A.; Hautdidier, B.; Gassiat, A.; Point, P.; Sautour, B.; et al. Bref Panorama Scientifique de L'estuaire de la Gironde. 2018. Available online: hal.inrae.fr/hal-02609253 (accessed on 24 January 2022).
49. Carvalho, A.N.; Santos, P.T. Factors affecting the distribution of epibenthic biodiversity in the Cávado estuary (NW Portugal). *Rev. Gest. Costeira Integr.* **2013**, *13*, 101–111. [CrossRef]
50. Gameiro, C.; Brotas, V. Patterns of Phytoplankton Variability in the Tagus Estuary (Portugal). *Estuaries Coasts* **2010**, *33*, 311–323. [CrossRef]
51. Silva, A.; Palma, S.; Oliveira, P.B.; Moita, M.T. Composition and interannual variability of phytoplankton in a coastal upwelling region (Lisbon Bay, Portugal). *J. Sea Res.* **2009**, *62*, 238–249. [CrossRef]
52. GIP Seine-Aval (Groupement d'Intérêt Public Seine-Aval). 2021. Available online: https://www.seine-aval.fr (accessed on 24 January 2022).
53. Amara, R.; Lagardere, F.; Desaunay, Y.; Marchand, J. Metamorphosis and estuarine colonisation in the common sole, *Solea solea* (L.): Implications for recruitment regulation. *Oceanol. Acta* **2000**, *23*, 469–484. [CrossRef]
54. Marn, N.; Jusup, M.; Legović, T.; Kooijman, S.A.L.M.; Klanjšček, T. Environmental effects on growth, reproduction, and life-history traits of loggerhead turtles. *Ecol. Model.* **2017**, *360*, 163–178. [CrossRef]
55. Pecquerie, L.; Petitgas, P.; Kooijman, S.A.L.M. Modeling fish growth and reproduction in the context of the Dynamic Energy Budget theory to predict environmental impact on anchovy spawning duration. *J. Sea Res.* **2009**, *62*, 93–105. [CrossRef]
56. Pethybridge, H.; Roos, D.; Loizeau, V.; Pecquerie, L.; Bacher, C. Responses of European anchovy vital rates and population growth to environmental fluctuations: An individual-based modeling approach. *Ecol. Model.* **2013**, *250*, 370–383. [CrossRef]
57. Stubbs, J.L.; Marn, N.; Vanderklift, M.A.; Fossette, S.; Mitchell, N.J. Simulated growth and reproduction of green turtles (*Chelonia mydas*) under climate change and marine heatwave scenarios. *Ecol. Model.* **2020**, *431*, 109185. [CrossRef]
58. Yúfera, M.; Parra, G.; Santiago, R.; Carrascosa, M. Growth, carbon, nitrogen and caloric content of *Solea senegalensis* (Pisces: *Soleidae*) from egg fertilization to metamorphosis. *Mar. Biol.* **1999**, *134*, 43–49. [CrossRef]
59. Marn, N.; Lika, K.; Augustine, S.; Goussen, B.; Ebeling, M.; Heckmann, D.; Gergs, A. Energetic basis for bird ontogeny and egg-laying applied to the bobwhite quail. *Conserv. Physiol.* **2022**, *10*, coac063. [CrossRef]
60. Augustine, S.; Litvak, M.K.; Kooijman, S.A.L.M. Stochastic feeding of fish larvae and their metabolic handling of starvation. *J. Sea Res.* **2011**, *66*, 411–418. [CrossRef]
61. Cabral, H. Differences in growth rates of juvenile *Solea solea* and *Solea senegalensis* in the Tagus estuary, Portugal. *J. Mar. Biol. Assoc. U. K.* **2003**, *83*, 861–868. [CrossRef]
62. Teixeira, C.M.; Cabral, H.N. Comparative analysis of the diet, growth and reproduction of the soles, *Solea solea* and *Solea senegalensis*, occurring in sympatry along the Portuguese coast. *J. Mar. Biol. Assoc. U. K.* **2010**, *90*, 995–1003. [CrossRef]
63. Tanner, S.E.; Teles-Machado, A.; Martinho, F.; Peliz, Á.; Cabral, H.N. Modelling larval dispersal dynamics of common sole (*Solea solea*) along the western Iberian coast. *Prog. Oceanogr.* **2017**, *156*, 78–90. [CrossRef]
64. Moreira, J.M.; Mendes, A.C.; Maulvault, A.L.; Marques, A.; Rosa, R.; Pousão-Ferreira, P.; Sousa, T.; Anacleto, P.; Marques, G.M. Impacts of ocean warming and acidification on the energy budget of three commercially important fish species. *Conserv. Physiol.* **2022**, *10*, coac048. [CrossRef]
65. Kooijman, S.A.L.M. What the hen can tell about her eggs: Egg development on the basis of energy budgets. *J. Math. Biol.* **1986**, *23*, 163–185. [CrossRef]
66. Devauchelle, N.; Alexandre, J.C.; Le Corre, N.; Letty, Y. Spawning of sole (*Solea solea*) in capivity. *Aquaculture* **1987**, *66*, 125–147. [CrossRef]
67. Jusup, M.; Klanjšček, T.; Matsuda, H. Simple measurements reveal the feeding history, the onset of reproduction, and energy conversion efficiencies in captive bluefin tuna. *J. Sea Res.* **2014**, *94*, 144–155. [CrossRef]
68. Cabral, H.N.; Costa, M.J.; Vinagre, C.; Pimentel, M.S.; Narciso, L.; Rosa, R. Contrasting impacts of climate change across seasons: Effects on flatfish cohorts. *Reg. Environ. Change* **2012**, *13*, 853–859. [CrossRef]
69. Pimentel, M.S.; Faleiro, F.; Dionisio, G.; Repolho, T.; Pousao-Ferreira, P.; Machado, J.; Rosa, R. Defective skeletogenesis and oversized otoliths in fish early stages in a changing ocean. *J. Exp. Biol.* **2014**, *217*, 2062–2070. [CrossRef]
70. Atkinson, D. Temperature and Organism Size—A Biological Law for Ectotherms? *Adv. Ecol. Res.* **1994**, *25*, 1–58. [CrossRef]
71. Levangie, P.E.L.; Blanchfield, P.J.; Hutchings, J.A. The influence of ocean warming on the natural mortality of marine fishes. *Environ. Biol. Fishes* **2021**, *105*, 1447–1461. [CrossRef]
72. Pauly, D. A framework for latitudinal comparisons of flatfish recruitment. *Neth. J. Sea Res.* **1994**, *32*, 107–118. [CrossRef]

73. Pauly, D. The gill-oxygen limitation theory (GOLT) and its critics. *Sci. Adv.* **2021**, *7*, eabc6050. [CrossRef] [PubMed]
74. Lefevre, S.; McKenzie, D.J.; Nilsson, G.E. In modelling effects of global warming, invalid assumptions lead to unrealistic projections. *Glob. Change Biol.* **2018**, *24*, 553–556. [CrossRef] [PubMed]
75. Miller, J.M.; Burke, J.S.; Fitzhugh, G.R. Early life history patterns of Atlantic North American flatfish: Likely (and unlikely) factors controlling recruitment. *Neth. J. Sea Res.* **1991**, *27*, 261–275. [CrossRef]
76. Rijnsdorp, A.D.; Vingerhoed, B. The ecological significance of geographical and seasonal differences in egg size in sole *Solea solea* (L.). *Neth. J. Sea Res.* **1994**, *32*, 255–270. [CrossRef]
77. Rickman, S.J.; Dulvy, N.K.; Jennings, S.; Reynolds, J.D. Recruitment variation related to fecundity in marine fishes. *Can. J. Fish. Aquat. Sci.* **2000**, *57*, 116–124. [CrossRef]
78. Verberk, W.C.E.P.; Atkinson, D.; Hoefnagel, K.N.; Hirst, A.G.; Horne, C.R.; Siepel, H. Shrinking body sizes in response to warming: Explanations for the temperature–size rule with special emphasis on the role of oxygen. *Biol. Rev.* **2021**, *96*, 247–268. [CrossRef]
79. Pankhurst, N.W.; Munday, P.L. Effects of climate change on fish reproduction and early life history stages. *Mar. Freshw. Res.* **2011**, *62*, 1015. [CrossRef]
80. Fiksen, Ø.; Jørgensen, C. Model of optimal behaviour in fish larvae predicts that food availability determines survival, but not growth. *Mar. Ecol. Prog. Ser.* **2011**, *432*, 207–219. [CrossRef]
81. Dou, S.Z.; Masuda, R.; Tanaka, M.; Tsukamoto, K. Effects of temperature and delayed initial feeding on the survival and growth of Japanese flounder larvae. *J. Fish Biol.* **2005**, *66*, 362–377. [CrossRef]
82. Bochdansky, A.B.; Grønkjær, P.; Herra, T.P.; Leggett, W.C. Experimental evidence for selection against fish larvae with high metabolic rates in a food limited environment. *Mar. Biol.* **2005**, *147*, 1413–1417. [CrossRef]
83. Pepin, P.; Robert, D.; Bouchard, C.; Dower, J.F.; Falardeau, M.; Fortier, L.; Jenkins, G.P.; Leclerc, V.; Levesque, K.; Llopiz, J.K.; et al. Once upon a larva: Revisiting the relationship between feeding success and growth in fish larvae. *ICES J. Mar. Sci.* **2014**, *72*, 359–373. [CrossRef]
84. Carballo, C.; Firmino, J.; Anjos, L.; Santos, S.; Power, D.M.; Manchado, M. Short- and long-term effects on growth and expression patterns in response to incubation temperatures in Senegalese sole. *Aquaculture* **2018**, *495*, 222–231. [CrossRef]
85. Dahlke, F.T.; Wohlrab, S.; Butzin, M.; Pörtner, H.O. Thermal bottlenecks in the life cycle define climate vulnerability of fish. *Science* **2020**, *369*, 65–70. [CrossRef]
86. Pörtner, H.O.; Knust, R. Climate change affects marine fishes through the oxygen limitation of thermal tolerance. *Science* **2007**, *315*, 95–97. [CrossRef]
87. Teske, P.R.; Sandoval-Castillo, J.; Golla, T.R.; Emami-Khoyi, A.; Tine, M.; von der Heyden, S.; Beheregaray, L.B. Thermal selection as a driver of marine ecological speciation. *Proc. R. Soc. B Biol. Sci.* **2019**, *286*, 20182023. [CrossRef]
88. Van Der Veer, H.W.; Kooijman, S.A.L.M.; van der Meer, J. Body size scaling relationships in flatfish as predicted by Dynamic Energy Budgets (DEB theory): Implications for recruitment. *J. Sea Res.* **2003**, *50*, 257–272. [CrossRef]
89. Ijima, H.; Jusup, M.; Takada, T.; Akita, T.; Matsuda, H.; Klanjscek, T. Effects of environmental change and early-life stochasticity on Pacific bluefin tuna population growth. *Mar. Environ. Res.* **2019**, *149*, 18–26. [CrossRef]
90. van de Wolfshaar, K.E.; Barbut, L.; Lacroix, G. From spawning to first-year recruitment: The fate of juvenile sole growth and survival under future climate conditions in the North Sea. *ICES J. Mar. Sci.* **2022**, *79*, 495–505. [CrossRef]
91. Barbut, L.; Groot Crego, C.; Delerue-Ricard, S.; Vandamme, S.; Volckaert, F.A.M.; Lacroix, G. How larval traits of six flatfish species impact connectivity. *Limnol. Oceanogr.* **2019**, *64*, 1150–1171. [CrossRef]
92. Galois, R.; Lagardre, F.; Richard, P. Changes in biochemical composition and otolith microstructure of larval common soleas, *Solea solea* (L.) under experimental starvation. *La Mer* **1990**, *28*, 273–285.
93. Deniel, C. Les Poissons Plats [Teleosteens, Pleuronectiformes] en Baie de Douarnenez: Reproduction, Croissance et Migration. Ph.D. Thesis, Universite de Bretagne Occidentale, Brest, France, 1981.
94. Mollet, F.; Kraak, S.; Rijnsdorp, A. Fisheries-induced evolutionary changes in maturation reaction norms in North sea sole *Solea solea*. *Mar. Ecol. Prog. Ser.* **2007**, *351*, 189–199. [CrossRef]
95. Dorel, D. Poissons de l Atlantique Nord-Est: Relations Taille-Poids. IFREMER. 1986. Available online: https://archimer.ifremer.fr/doc/00000/1289/ (accessed on 1 December 2022).
96. Wheeler, A. *Key to the Fishes of Northern Europe*; Food and Agriculture Organization of the United Nations: Rome, Italy, 1978.
97. Witthames, P.; Greer Walker, M. Determinacy of fecundity and oocyte atresia in sole (*Solea solea*) from the Channel, the North Sea and the Irish Sea). *Aquat. Living Resour.* **1995**, *8*, 91–109. [CrossRef]
98. Fonds, M.; Drinkwaard, B.; Resink, J.W.; Eysink, G.G.J.; Toet, W. Measurements of metabolism, food intake and growth of *Solea solea* (L.) fed with mussel meat or with dry food. *Aquac. A Biotechnol. Prog.* **1989**, *2*, 1851–1874.
99. Lund, I.; Steenfeldt, S.J.; Suhr, K.I.; Hansen, B.W. A comparison of fatty acid composition and quality aspects of eggs and larvae from cultured and wild broodstock of common sole (*Solea solea*, L.). *Aquac. Nutr.* **2008**, *14*, 544–555. [CrossRef]
100. Teal, L. IMARES Data Base Frisbe. 2011. Available online: http://www.bio.vu.nl/thb/deb/deblab/add_my_pet/entries_web/Solea_solea/Solea_solea_res.html (accessed on 15 January 2022).
101. Vinagre, C. Ecology of the Juveniles of the Soles *Solea solea* (Linnaeus, 1758) and *Solea senegalensis* (Kaup, 1858), in the Tagus Estuary. Ph.D. Thesis, University of Lisbon, Lisbon, Portugal, 2007.
102. Manchado, M. IFAPA Centro El Toruño, Junta de Andalucía, Camino Tiro Pichón s/n, 11500 El Puerto de Santa Maria, Spain. Personal Communication, Unpublished Work. 2021.

103. Ribeiro, L.; Sarasquete, C.; Dinis, M.T. Histological and histochemical development of the digestive system of *Solea senegalensis* (Kaup, 1858) larvae. *Aquaculture* **1999**, *171*, 293–308. [CrossRef]
104. Parra, G.; Yufera, M. Comparative energetics during early development of two marine fish species, *Solea senegalensis* (Kaup) and *Sparus aurata* (L.). *J. Exp. Biol.* **2001**, *204 Pt 12*, 2175–2183. [CrossRef]
105. Canavate, J.P.; Fernandez-Diaz, C. Influence of co-feeding larvae with live and inert diets on weaning the sole *Solea senegalensis* onto commercial dry feeds. *Aquaculture* **1999**, *174*, 255–263. [CrossRef]
106. Ribeiro, L.; Engrola, S.; Dinis, M.T. Weaning of Senegalese sole (*Solea senegalensis*) postlarvae to an inert diet with a co-feeding regime. *Cienc. Mar.* **2017**, *31*, 327–337. [CrossRef]
107. Ortiz-Delgado, J.B.; Funes, V.; Sarasquete, C. The organophosphate pesticide-{OP}-malathion inducing thyroidal disruptions and failures in the metamorphosis of the Senegalese sole, *Solea senegalensis*. *BMC Vet. Res.* **2019**, *15*, 57. [CrossRef] [PubMed]
108. Maulvault, A.L.; Marques, A.; Rosa, R.; Mendes, A.; Pousao-Ferreira, P.; Anacleto, P. Experimental data from {MARE}, University of Lisbon, Lisbon, Portugal. For Using This Data Outside of the Script before Publication Please Contact Jose Moreira (j.miguel.moreira@tecnico.ulisboa.pt) or Patricia Anacleto (panacleto@ipma.pt). Unpublished Work. 2019.

Disclaimer/Publisher's Note: The statements, opinions and data contained in all publications are solely those of the individual author(s) and contributor(s) and not of MDPI and/or the editor(s). MDPI and/or the editor(s) disclaim responsibility for any injury to people or property resulting from any ideas, methods, instructions or products referred to in the content.